AIMS Mathematics, 11(10): 35429–35468.
DOI: 10.3934/math.20261375
Received: 03 August 2026
Revised: 26 September 2026
Accepted: 10 October 2026
Published: 28 October 2026

http://www.aimspress.com/journal/Math

Research article

The Ujlayan-Dixit fractional Weibull distribution: statistical properties, estimation, and applications to engineering and biomedical data

Nesreen M. Al-Olaimat[1,*], Hatim Solayman Migdadi[2], Afaf Alrashidi[3] and Samirah Alzubaidi[4]

[1] Department of Applied Science, Ajloun College, Al-Balqa Applied University, Ajloun 26816, Jordan

[2] Department of Mathematics, Faculty of Science, The Hashemite University, Zarqa 13133, Jordan

[3] Department of Statistics, Faculty of Science, University of Tabuk, Tabuk, Saudi Arabia

[4] Department of Mathematics, Al-Qunfudah University College, Umm Al-Qura University, Mecca, Saudi Arabia

* **Correspondence:** Email: n.malolaimat@bau.edu.jo.

Abstract: A new three-parameter Ujlayan-Dixit fractional Weibull distribution (UDFWD) is proposed by replacing the ordinary derivative in the differential equation generating the classical Weibull density with the Ujlayan-Dixit fractional (UDF) derivative of order $q \in (0, 1]$. The resulting density is expressed as a convergent infinite series involving the gamma function. Series representations are obtained for the cumulative distribution, survival, and hazard rate functions in terms of the lower and upper incomplete gamma functions, together with sufficient conditions on (θ, β, q) for absolute convergence. Unlike most Weibull-type extensions, whose aging behavior is examined only numerically, the proposed density is proved to be strictly log-concave for $\theta > 1, \beta > 0$, and $0 < q \leq 1$. The UDFWD therefore has a strictly increasing hazard rate and a unique mode, and the fractional parameter is shown to govern the level and the growth of the hazard through the factor $1/q$ and the additive constant $(1 - q)/q$. Several structural properties are also derived, including the mode; the quantile function; the ordinary moments; and the Shannon, Tsallis, and Rényi entropies. The unknown parameters are estimated using the maximum likelihood, least squares, and weighted least squares methods, and a Monte Carlo simulation study provides numerical evidence that the mean square errors (MSEs) and absolute relative biases generally decrease as the sample size increases, with the maximum likelihood method attaining the smallest MSEs in most settings with moderate and large sample sizes. Finally, two real datasets, on carbon fiber tensile strength and serum creatinine, show that the UDFWD attains the smallest values of all model-selection criteria against six competing lifetime models, while remaining highly competitive on the distance-based goodness-of-fit measures.

Keywords: Ujlayan-Dixit fractional derivative; Weibull distribution; hazard rate function; log-concavity; maximum likelihood estimation; moments and entropy; Monte Carlo simulation
Mathematics Subject Classification: 26A33, 60E05, 62N05, 62F10

1. Introduction

Continuous positive data arise frequently in reliability engineering, survival analysis, and biomedical studies. Examples include failure times of engineering components, tensile strengths of materials, survival times, and biomedical measurements; see [1, 2]. Such data may exhibit different levels of skewness and tail behavior. Hence, selecting an adequate probability distribution is essential for describing these data and drawing reliable statistical inferences.

Among lifetime distributions, the Weibull distribution (WD) introduced by Weibull [3] is one of the most widely used models. Its popularity is mainly due to its simple mathematical form and its ability to represent decreasing, constant, and increasing hazard rates through its shape parameter. However, the classical WD has only two parameters. As a result, its density shape, tail behavior, and hazard growth are tightly linked. This may limit its ability to fit some positive continuous datasets. For this reason, more flexible Weibull-type models have been developed.

In the recent past, many generalizations of the WD have been proposed. Notable among them are the exponentiated WD introduced by Mudholkar and Srivastava [4] and the modified WD studied by Lai et al. [5]. A new extension of the odd inverse WD family of distributions was studied by Abdelall et al. [6]. Bebbington et al. [7] proposed the flexible Weibull extension, and Ghitany et al. [8] obtained the Marshall-Olkin extended WD. Cordeiro et al. [9] introduced the Kumaraswamy WD, Aryal and Tsokos [10] proposed the transmuted WD, and Nassar et al. [11] studied the alpha-power WD. These models add new parameters or transformations to the baseline, so that the density and the hazard can take more flexible shapes.

Other Weibull-type models have appeared more recently. Shama et al. [12] proposed the modified generalized WD, and Alshanbari et al. [13] introduced a flexible Weibull extension model. Emam [14] obtained the generalized Weibull-Weibull distribution. Moreover, the modified alpha-power transformed WD was investigated by Alotaibi et al. [15], and the flexible Weibull extension was modeled within the generalized additive model for location, scale, and shape (GAMLSS) framework by Hernández-Barajas et al. [16]. Additionally, Afify et al. [17] introduced the generalized Kavya-Manoharan Weibull distribution and investigated its statistical properties. They also considered eight parameter estimation methods and assessed the performance of the proposed model using three real datasets. Studies of this kind add to the continued development of Weibull-based models, moving toward greater flexibility in representing probability distributions.

Fractional differential equations offer another way to generate new probability distributions. In this method, the ordinary derivative appearing in the differential equation associated with a classical density is replaced by a fractional derivative. The resulting differential equation is then solved to obtain a new distribution that contains an additional fractional parameter. The generalization is therefore obtained from the mechanism that generates the density, and the classical model is recovered exactly when the fractional order equals one.

Several fractional operators have been employed toward this end. The derivatives Riemann-Liouville and Caputo, both nonlocal and integral, underlie a substantial body of work on probability distributions and stochastic-process models [18–20]. A relatively recent line of research relies instead on local operators. Among these is the conformable derivative, which, for differentiable functions, reduces to a pointwise rescaling of the ordinary derivative, that is, multiplication by a factor that depends on both the point of evaluation and the fractional order. It has also been used as a basis

for constructing fractional probability distributions [21].

Following this local-operator approach, the present study develops the UDFWD using the Ujlayan-Dixit (UD) operator. In this study, we replace the ordinary derivative in the differential equation satisfied by the classical Weibull probability density function with the UD operator defined below. The resulting extension is obtained through the differential equation itself, rather than by directly modifying the PDF or CDF. Since the terms arising from this substitution depend on the same model parameters, their coefficients cannot be adjusted independently. The construction is concerned with the probability distribution itself. We neither assume nor derive an underlying stochastic process.

Dixit et al. [22] introduced the Ujlayan-Dixit fractional (UDF) derivative used in this study, which was further examined by Dixit and Ujlayan [23]. For a given function $g : [0, \infty) \to \mathbb{R}$ and $q \in [0, 1]$, the UD derivative of order q is defined by

$$D^q g(x) = \lim_{\varepsilon \to 0} \frac{e^{\varepsilon(1-q)} g\left(xe^{\frac{\varepsilon q}{x}}\right) - g(x)}{\varepsilon}, \tag{1.1}$$

provided that the limit exists. If g is differentiable, then the UD derivative takes the form

$$D^q g(x) = (1 - q)g(x) + qg'(x). \tag{1.2}$$

The operator in (1.2) admits a direct interpretation: It combines the value of the function at the point under consideration with its local rate of change, which is represented by the ordinary derivative; see [24]. Unlike the ordinary derivative, which describes only the instantaneous local rate of change, the UD operator also includes a term involving the function value. The relative contributions of these two components are determined by the parameter q. For small values of q, greater weight is assigned to the function-value term, whereas the ordinary derivative becomes more influential as q approaches one. In lifetime modeling, q may therefore be regarded as a dimensionless deformation parameter indicating the departure from the classical WD. This departure is reflected in the concentration and tail behavior of the distribution, as well as in the level and growth of the hazard rate in lifetime-data applications.

It is worth noting that both weights, $1 - q$ and q, are non-negative for $0 < q < 1$. The value $q = 0$ is excluded because the Ujlayan-Dixit fractional Weibull distribution (UDFWD) involves terms in $1/q$; orders greater than one are not covered by the UD operator considered in this paper. At $q = 1$, however, the UD derivative coincides with the ordinary derivative, and the classical WD is recovered. Thus, $q = 1$ is included as a boundary case of the UDFWD model family. Throughout the theoretical development, $q \in (0, 1]$, and $q \to 1^-$ denotes convergence to this boundary from the fractional interior $0 < q < 1$.

In recent years, the UD derivative has been used to generate several fractional probability distributions. Alhribat and Samuh [24] presented a general method for obtaining new distributions from fractional differential equations. Jamal et al. [25] developed this approach further. Al-Olaimat et al. [26] applied the UD derivative to the Lomax distribution. In each of these studies, the fractional order enters as an additional parameter, and the classical model is recovered at the boundary of the extended family.

For completeness, let X follow the classical WD with shape parameter $\theta > 0$ and rate parameter $\beta > 0$. Then, its cumulative distribution, the corresponding probability density, the survival, and the

hazard functions are respectively given by

$$F(x;\theta,\beta) = 1 - e^{-\beta x^{\theta}}, \qquad x > 0, \tag{1.3}$$

$$f(x;\theta,\beta) = \theta\beta x^{\theta-1} e^{-\beta x^{\theta}}, \qquad x > 0, \tag{1.4}$$

$$S(x;\theta,\beta) = e^{-\beta x^{\theta}}, \qquad x > 0, \tag{1.5}$$

$$h(x;\theta,\beta) = \theta\beta x^{\theta-1}, \qquad x > 0. \tag{1.6}$$

To the best of our knowledge, no UDF extension of the WD has been proposed. Motivated by this gap, the UDFWD is proposed. This model is obtained by replacing the ordinary derivative in the first-order differential equation associated with the classical Weibull density by the UDF derivative of order $q \in (0, 1]$.

Two contributions may be distinguished here. Mathematically, the paper presents the UD-based construction and an analytical characterization of the resulting aging properties. Practically, it offers the interpretable hazard flexibility introduced by q, along with the competitive empirical performance of the resulting model.

The main contributions of this paper are summarized as follows:
(1) The UDFWD is derived as the solution of a UD-fractional differential equation, and a series representation of its normalizing constant is obtained. The absolute convergence of the resulting series is established, and the classical WD is recovered when $q \to 1^{-}$.
(2) Series expressions for the cumulative distribution, survival, and hazard functions are derived in terms of the gamma and incomplete gamma functions. Some important statistical properties, including the mode; the quantile function; the ordinary moments; and the Shannon, Tsallis, and Rényi entropy measures, are also obtained.
(3) The density is proved to be strictly log-concave for $\theta > 1$, $\beta > 0$, and $0 < q \leq 1$, so that the UDFWD has a strictly increasing hazard rate and a unique mode. The fractional parameter governs the level and the growth of the hazard through the factor $1/q$ and the additive constant $(1 - q)/q$.
(4) The unknown parameters are estimated using different estimation methods. Moreover, a Monte Carlo simulation study is conducted to assess the finite-sample performance of the estimators using the average estimates, relative biases, and mean squared errors.
(5) The practical performance of the UDFWD is examined using two real datasets representing carbon fiber tensile strength and serum creatinine levels.

The remainder of the paper is organized as follows. Section 2 introduces the UDFWD and derives its probability density, cumulative distribution, survival, and hazard functions, as well as its log-concavity and monotone hazard property. Section 3 presents some statistical properties of the proposed model, including the mode, quantile function, moments, and entropy measures. Section 4 discusses the maximum likelihood, least squares, and weighted least squares estimation methods and presents the Monte Carlo simulation study. Section 5 provides the real-data applications, and Section 6 concludes the paper.

2. The Ujlayan-Dixit fractional Weibull distribution

This section introduces the UDFWD. The proposed model is obtained by rewriting the classical WD as the solution of a first-order ordinary differential equation and then replacing the ordinary derivative with the UDF derivative.

2.1. Derivation of the probability density function

From Eq (1.4), differentiating with respect to x and rearranging the resulting expression gives

$$f'(x;\theta,\beta) = \left[\frac{\theta-1}{x} - \beta\theta x^{\theta-1}\right] f(x;\theta,\beta),$$

or equivalently,

$$f'(x;\theta,\beta) + \left[\beta\theta x^{\theta-1} - \frac{\theta-1}{x}\right] f(x;\theta,\beta) = 0.$$

This is the first-order ordinary differential equation associated with the classical Weibull density. To obtain the UDF form, the ordinary derivative is replaced by the UDF derivative. Hence,

$$D^q f(x) + \left[\beta\theta x^{\theta-1} - \frac{\theta-1}{x}\right] f(x) = 0.$$

Using Eq (1.2), the preceding equation becomes

$$f'(x) + \left[\frac{1-q}{q} + \frac{\beta\theta}{q}x^{\theta-1} - \frac{\theta-1}{qx}\right] f(x) = 0.$$

Solving this first-order linear differential equation, we obtain

$$f_q(x;\theta,\beta,q) = C\, x^{\frac{\theta-1}{q}} e^{-\frac{1-q}{q}x - \frac{\beta}{q}x^{\theta}}, \qquad x > 0, \tag{2.1}$$

where C is the normalizing constant. Because

$$\int_0^\infty f_q(x;\theta,\beta,q)\, dx = 1,$$

substituting Eq (2.1) gives the following expression for the normalizing constant:

$$C^{-1} = \int_0^\infty x^{\frac{\theta-1}{q}} e^{-\frac{1-q}{q}x - \frac{\beta}{q}x^{\theta}}\, \mathrm{d}x. \tag{2.2}$$

Integrability of the density holds for $\beta > 0$, $0 < q \le 1$, and $\theta > 1 - q$. Convergence of the infinite series in the normalizing constant calls for the stronger requirement $\theta > 1$, which is imposed here. In the intermediate range $0 < q < 1$ with $1 - q < \theta \le 1$, the density is still well defined through the integral representation in Eq (2.2). However, the series representation is no longer guaranteed, together with the increasing-hazard results developed below. Parameter values of this type are by no means unimportant in reliability work, where constant or decreasing failure-rate behavior may be the phenomenon of interest, and Eq (2.2) can then be evaluated numerically. The closed-form development that follows is accordingly carried out under $\theta > 1, \beta > 0$, and $0 < q \le 1$.

Remark 2.1. *The decomposition in Eq* (2.1)*, term by term, shows what the UD construction contributes. The term* $(1 - q)f(x)$ *in the UD derivative is responsible for the additional exponential factor*

$$e^{\frac{-(1-q)x}{q}},$$

and the Weibull terms of the original differential equation account for the factor

$$e^{\frac{-\beta x^{\theta}}{q}}$$

together with the power prefactor

$$x^{\frac{(\theta-1)}{q}}.$$

Exponential decay and a power prefactor therefore coexist as a direct consequence of the modified differential equation and not as the outcome of a transformation applied to the Weibull density.

Together with the integrability condition established above, this shows that the UD replacement modifies the density-generating mechanism while still yielding a well-defined parametric probability model, rather than serving only as a formal modification of the differential equation associated with the classical Weibull density.

2.1.1. Closed-form series representation of the normalizing constant

For $0 < q < 1$, using the series expansion

$$e^{-\frac{1-q}{q}x} = \sum_{j=0}^{\infty} \frac{(-\frac{1-q}{q}x)^j}{j!}$$

and substituting it into Eq (2.2), we obtain

$$C^{-1} = \int_0^{\infty} x^{\frac{\theta-1}{q}} e^{-\frac{\beta}{q}x^{\theta}} \sum_{j=0}^{\infty} \frac{(-\frac{1-q}{q}x)^j}{j!}\, dx.$$

Under the condition $\theta > 1$, the corresponding series is absolutely convergent. Therefore, the order of summation and integration can be interchanged, yielding

$$C^{-1} = \sum_{j=0}^{\infty} \frac{(-\frac{1-q}{q})^j}{j!} \int_0^{\infty} x^{\frac{\theta-1}{q}+j} e^{-\frac{\beta}{q}x^{\theta}}\, dx.$$

Using the substitution

$$u = \frac{\beta}{q}x^{\theta},$$

we have

$$\int_0^{\infty} x^{\frac{\theta-1}{q}+j} e^{-\frac{\beta}{q}x^{\theta}}\, dx = \frac{1}{\theta}\left(\frac{\beta}{q}\right)^{-\frac{\theta+q(j+1)-1}{q\theta}} \Gamma\left(\frac{\theta+q(j+1)-1}{q\theta}\right).$$

Consequently, the normalizing constant is

$$C = \frac{\theta\left(\frac{\beta}{q}\right)^{\frac{\theta+q-1}{q\theta}}}{\sum_{j=0}^{\infty} \frac{\left[-\frac{1-q}{q}\left(\frac{\beta}{q}\right)^{-\frac{1}{\theta}}\right]^j}{j!} \Gamma\left(\frac{\theta+q(j+1)-1}{q\theta}\right)}. \tag{2.3}$$

Therefore, the probability density function (PDF) of the UDFWD is given by

$$f_q(x;\theta,\beta,q) = \frac{\theta\left(\frac{\beta}{q}\right)^{\frac{\theta+q-1}{q\theta}} x^{\frac{\theta-1}{q}} e^{-\frac{1-q}{q}x-\frac{\beta}{q}x^{\theta}}}{\sum_{j=0}^{\infty}\frac{\left[-\frac{1-q}{q}\left(\frac{\beta}{q}\right)^{-\frac{1}{\theta}}\right]^{j}}{j!}\Gamma\left(\frac{\theta+q(j+1)-1}{q\theta}\right)}, \qquad x>0. \tag{2.4}$$

Therefore, if X has the PDF given in Eq (2.4), we write

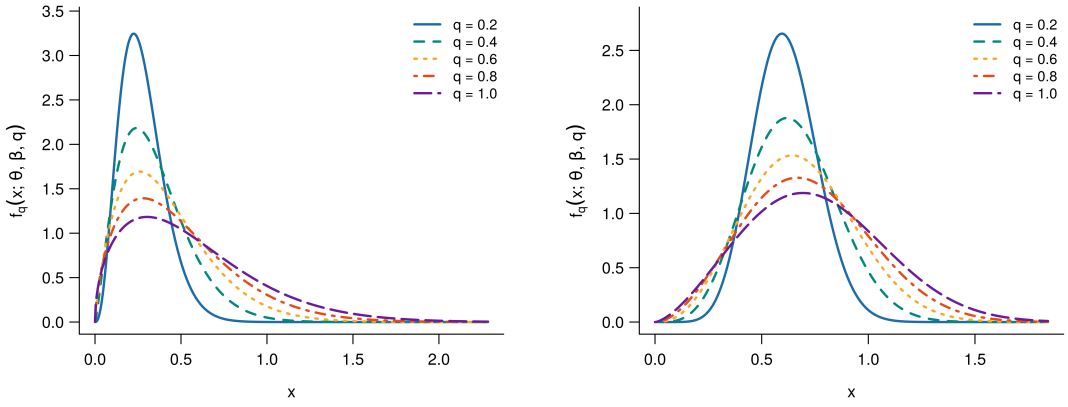
$$X \sim \text{UDFWD}(\theta,\beta,q), \qquad \theta>1, \quad \beta>0, \quad 0<q\leq 1.$$

The infinite series defining the normalizing constant in Eq (2.3) is absolutely convergent for $\theta > 1$; the proof is provided in Appendix A. Moreover, as $q \to 1^-$, we have $(1-q)/q \to 0$, $\beta/q \to \beta$, and only the term corresponding to $j = 0$ remains in the denominator of Eq (2.4). Therefore,

$$\lim_{q\to 1^-} f_q(x;\theta,\beta,q) = \theta\beta x^{\theta-1}e^{-\beta x^{\theta}}.$$

Thus, the classical WD is recovered as a special case.

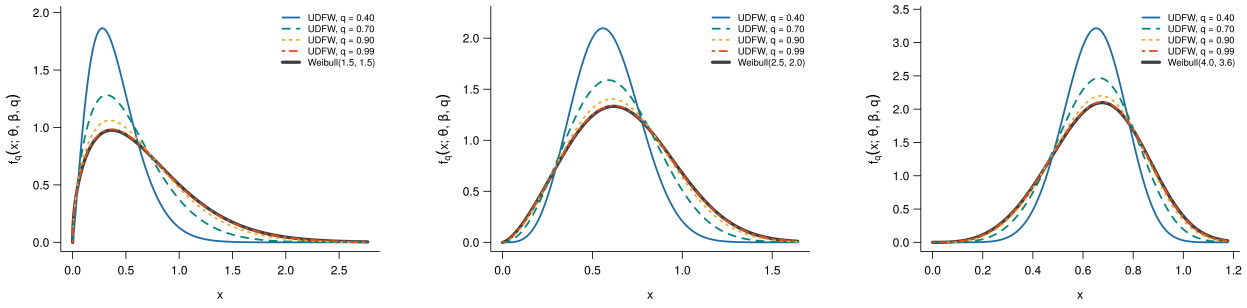
To illustrate the effect of the fractional parameter q on the shape of the UDFWD density, Figure 1 presents the PDF for selected values of q under two parameter settings. The plots show that decreasing q raises the modal height and concentrates the density around its mode, whereas increasing q flattens the density and lengthens the right tail; the case $q = 1$ corresponds to the WD.



(a) $\theta = 1.5, \beta = 2.$ **(b)** $\theta = 2.5, \beta = 1.5.$

Figure 1. PDF curves of the UDFWD for selected values of q: (a) $\theta = 1.5, \beta = 2$; (b) $\theta = 2.5$, $\beta = 1.5$.

Figure 2 illustrates the convergence of the UDFWD density to the classical Weibull density as $q \to 1^-$ under different values of θ and β. In each case, the UDFWD curve approaches the corresponding WD curve monotonically, and the two curves are practically indistinguishable at $q = 0.99$.



(a) $\theta = 1.5, \beta = 1.5$. **(b)** $\theta = 2.5, \beta = 2$. **(c)** $\theta = 4, \beta = 3.6$.

Figure 2. Convergence of the UDFWD PDF to the WD PDF as $q \to 1^-$.

2.2. *Cumulative distribution function*

Let $X \sim \text{UDFWD}(\theta, \beta, q)$. The cumulative distribution function (CDF) of X is defined by

$$F_q(x;\theta,\beta,q) = P(X \le x) = \int_0^x f_q(t;\theta,\beta,q)\,dt.$$

Using the density in Eq (2.4), the following expression is obtained:

$$F_q(x;\theta,\beta,q) = \frac{\theta\left(\frac{\beta}{q}\right)^{\frac{\theta+q-1}{q\theta}}}{\sum_{j=0}^{\infty}\frac{\left[-\frac{1-q}{q}\left(\frac{\beta}{q}\right)^{-\frac{1}{\theta}}\right]^j}{j!}\Gamma\left(\frac{\theta+q(j+1)-1}{q\theta}\right)}\int_0^x t^{\frac{\theta-1}{q}}e^{-\frac{1-q}{q}t-\frac{\beta}{q}t^\theta}\,dt.$$

For $0 < q < 1$, using the series expansion

$$e^{-\frac{1-q}{q}t} = \sum_{j=0}^{\infty}\frac{(-\frac{1-q}{q}t)^j}{j!},$$

substituting the preceding series expansion and interchanging the order of summation and integration yields:

$$F_q(x;\theta,\beta,q) = \frac{\theta\left(\frac{\beta}{q}\right)^{\frac{\theta+q-1}{q\theta}}}{\sum_{j=0}^{\infty}\frac{\left[-\frac{1-q}{q}\left(\frac{\beta}{q}\right)^{-\frac{1}{\theta}}\right]^j}{j!}\Gamma\left(\frac{\theta+q(j+1)-1}{q\theta}\right)}\sum_{j=0}^{\infty}\frac{\left(-\frac{1-q}{q}\right)^j}{j!}\int_0^x t^{\frac{\theta-1}{q}+j}e^{-\frac{\beta}{q}t^\theta}\,dt.$$

Using the substitution

$$u = \frac{\beta}{q}t^\theta,$$

the integral becomes:

$$\int_0^x t^{\frac{\theta-1}{q}+j}e^{-\frac{\beta}{q}t^\theta}\,dt = \frac{1}{\theta}\left(\frac{\beta}{q}\right)^{-\frac{\theta+q(j+1)-1}{q\theta}}\gamma\left(\frac{\theta+q(j+1)-1}{q\theta},\frac{\beta}{q}x^\theta\right).$$

Therefore, the CDF of the UDFWD is given by

$$F_q(x;\theta,\beta,q) = \frac{\displaystyle\sum_{j=0}^{\infty} \frac{\left[-\frac{1-q}{q}\left(\frac{\beta}{q}\right)^{-\frac{1}{\theta}}\right]^j}{j!}\gamma\left(\frac{\theta+q(j+1)-1}{q\theta}, \frac{\beta}{q}x^{\theta}\right)}{\displaystyle\sum_{j=0}^{\infty} \frac{\left[-\frac{1-q}{q}\left(\frac{\beta}{q}\right)^{-\frac{1}{\theta}}\right]^j}{j!}\Gamma\left(\frac{\theta+q(j+1)-1}{q\theta}\right)}, \qquad x > 0, \tag{2.5}$$

where $\gamma(a,z)$ is the lower incomplete gamma function, $\gamma(a,z) = \int_0^z u^{a-1}e^{-u}\,du$.

Moreover, when $q \to 1^-$, only the term corresponding to $j = 0$ remains. Hence,

$$\lim_{q\to 1^-} F_q(x;\theta,\beta,q) = 1 - e^{-\beta x^{\theta}}.$$

Thus, the CDF of the classical WD is recovered as a special case.

2.3. Survival function of the UDFWD

For $X \sim \text{UDFWD}(\theta,\beta,q)$, the survival function is defined by

$$S_q(x;\theta,\beta,q) = \int_x^{\infty} f_q(t;\theta,\beta,q)\,dt.$$

Using the PDF given in Eq (2.4), the survival function can be written as

$$S_q(x;\theta,\beta,q) = \frac{\theta\left(\frac{\beta}{q}\right)^{\frac{\theta+q-1}{q\theta}}}{\displaystyle\sum_{j=0}^{\infty} \frac{\left[-\frac{1-q}{q}\left(\frac{\beta}{q}\right)^{-\frac{1}{\theta}}\right]^j}{j!}\Gamma\left(\frac{\theta+q(j+1)-1}{q\theta}\right)} \int_x^{\infty} t^{\frac{\theta-1}{q}} e^{-\frac{1-q}{q}t-\frac{\beta}{q}t^{\theta}}\,dt.$$

For $0 < q < 1$, the exponential term has the series expansion

$$e^{-\frac{1-q}{q}t} = \sum_{j=0}^{\infty} \frac{(-\frac{1-q}{q}t)^j}{j!}.$$

Because the series of the corresponding absolute integrals is convergent for $\theta > 1$, the order of summation and integration can be interchanged. Thus,

$$S_q(x;\theta,\beta,q) = \frac{\theta\left(\frac{\beta}{q}\right)^{\frac{\theta+q-1}{q\theta}}}{\displaystyle\sum_{j=0}^{\infty} \frac{\left[-\frac{1-q}{q}\left(\frac{\beta}{q}\right)^{-\frac{1}{\theta}}\right]^j}{j!}\Gamma\left(\frac{\theta+q(j+1)-1}{q\theta}\right)} \sum_{j=0}^{\infty} \frac{\left(-\frac{1-q}{q}\right)^j}{j!} \int_x^{\infty} t^{\frac{\theta-1}{q}+j} e^{-\frac{\beta}{q}t^{\theta}}\,dt.$$

Using the substitution

$$u = \frac{\beta}{q}t^{\theta},$$

the integral becomes:

$$\int_x^{\infty} t^{\frac{\theta-1}{q}+j} e^{-\frac{\beta}{q}t^{\theta}}\, dt = \frac{1}{\theta}\Big(\frac{\beta}{q}\Big)^{-\frac{\theta+q(j+1)-1}{q\theta}} \Gamma\Big(\frac{\theta+q(j+1)-1}{q\theta}, \frac{\beta}{q}x^{\theta}\Big).$$

Therefore, the survival function of the UDFWD is given by

$$S_q(x;\theta,\beta,q) = \frac{\displaystyle\sum_{j=0}^{\infty} \frac{\left[-\frac{1-q}{q}\left(\frac{\beta}{q}\right)^{-\frac{1}{\theta}}\right]^j}{j!}\Gamma\left(\frac{\theta+q(j+1)-1}{q\theta}, \frac{\beta}{q}x^{\theta}\right)}{\displaystyle\sum_{j=0}^{\infty} \frac{\left[-\frac{1-q}{q}\left(\frac{\beta}{q}\right)^{-\frac{1}{\theta}}\right]^j}{j!}\Gamma\left(\frac{\theta+q(j+1)-1}{q\theta}\right)}, \qquad x > 0, \tag{2.6}$$

where $\Gamma(a,z)$ is the upper incomplete gamma function, $\Gamma(a,z) = \int_z^{\infty} u^{a-1}e^{-u}\, du$.

Moreover, when $q \to 1^-$, only the term corresponding to $j = 0$ remains in Eq (2.6). Because $\Gamma(1,z) = e^{-z}$, it follows that

$$\lim_{q\to 1^-} S_q(x;\theta,\beta,q) = e^{-\beta x^{\theta}}.$$

Thus, the survival function of the classical WD is recovered as a special case.

2.4. Hazard function of the UDFWD

For $X \sim \text{UDFWD}(\theta,\beta,q)$, the hazard function, denoted by $h_q(x;\theta,\beta,q)$, represents the instantaneous failure rate at time x, conditional on survival up to time x, and is defined by

$$h_q(x;\theta,\beta,q) = \frac{f_q(x;\theta,\beta,q)}{S_q(x;\theta,\beta,q)}, \qquad x > 0.$$

Substituting Eqs (2.4) and (2.6) into the preceding expression and canceling the common normalizing factor yields

$$h_q(x;\theta,\beta,q) = \frac{\theta\Big(\frac{\beta}{q}\Big)^{\frac{\theta+q-1}{q\theta}} x^{\frac{\theta-1}{q}} e^{-\frac{1-q}{q}x-\frac{\beta}{q}x^{\theta}}}{\displaystyle\sum_{j=0}^{\infty} \frac{\left[-\frac{1-q}{q}\left(\frac{\beta}{q}\right)^{-\frac{1}{\theta}}\right]^j}{j!}\Gamma\Big(\frac{\theta+q(j+1)-1}{q\theta}, \frac{\beta}{q}x^{\theta}\Big)}, \qquad x > 0, \tag{2.7}$$

where $\theta > 1, \beta > 0$, and $0 < q \le 1$.

Moreover, as $q \to 1^-$, only the term corresponding to $j = 0$ remains in Eq (2.7). Therefore,

$$\lim_{q\to 1^-} h_q(x;\theta,\beta,q) = \theta\beta x^{\theta-1}.$$

Thus, the hazard function of the classical WD is recovered as a special case.

2.5. Log-concavity and monotone hazard rate

Proposition 2.1. *Let $X \sim \mathrm{UDFWD}(\theta, \beta, q)$ with $\theta > 1$, $\beta > 0$, and $0 < q \leq 1$. Then:*
(i) *f_q is strictly log-concave on $(0, \infty)$;*
(ii) *h_q is strictly increasing on $(0, \infty)$, with $h_q(0^+) = 0$ and $h_q(x) \to \infty$ as $x \to \infty$;*
(iii) *as $x \to \infty$,*

$$h_q(x) = \frac{\beta\theta}{q}\, x^{\theta-1} + \frac{1-q}{q} + O\Big(x^{-1}\Big);$$

(iv) *Consequently, the UDFWD has an increasing failure rate (IFR), an increasing failure rate average (IFRA), new better than used (NBU), new better than used in expectation (NBUE), and decreasing mean residual life (DMRL); its density is strictly unimodal.*

Proof.
(i) From Eq (2.4), for $x > 0$,

$$\log f_q(x; \theta, \beta, q) = \log C + \frac{\theta - 1}{q} \log x - \frac{1-q}{q}\, x - \frac{\beta}{q}\, x^{\theta},$$

where C does not depend on x. Differentiating twice,

$$\frac{d^2}{dx^2} \log f_q(x) = -\frac{\theta - 1}{q\, x^2} - \frac{\beta\theta(\theta - 1)}{q}\, x^{\theta-2}.$$

For $\theta > 1$, $\beta > 0$, and $q \in (0, 1]$, both terms are strictly negative for every $x > 0$, so $\log f_q$ is strictly concave.
(ii) Strict log-concavity implies that for each fixed $t > 0$, the ratio

$$x \mapsto \frac{f_q(x + t)}{f_q(x)}$$

is strictly decreasing. Because

$$\frac{1}{h_q(x)} = \frac{S_q(x)}{f_q(x)} = \int_0^{\infty} \frac{f_q(x + t)}{f_q(x)}\, dt,$$

the integrand decreases in x for every t; hence, $1/h_q$ is strictly decreasing, and h_q is strictly increasing. Because $(\theta - 1)/q > 0$, we have $f_q(0^+) = 0$ and $S_q(0^+) = 1$, giving $h_q(0^+) = 0$.
(iii) Write $f_q(x) = e^{-\varphi(x)}$, where

$$\varphi(x) = -\log C - \frac{\theta - 1}{q} \log x + \frac{1-q}{q} x + \frac{\beta}{q} x^{\theta}.$$

Then,

$$\varphi'(x) = \frac{\beta\theta}{q}\, x^{\theta-1} + \frac{1-q}{q} - \frac{\theta - 1}{qx},$$

and

$$\varphi''(x) = \frac{\beta\theta(\theta - 1)}{q}\, x^{\theta-2} + \frac{\theta - 1}{qx^2}.$$

For sufficiently large x, $\varphi'(x) > 0$, integration by parts gives

$$S_q(x) = \frac{f_q(x)}{\varphi'(x)} - \int_x^\infty \frac{\varphi''(t)}{\{\varphi'(t)\}^2} f_q(t)\, dt.$$

Because

$$\frac{\varphi''(t)}{\{\varphi'(t)\}^2} = O(t^{-\theta}),$$

the integral remainder is $O\left(x^{-\theta} S_q(x)\right)$. Hence,

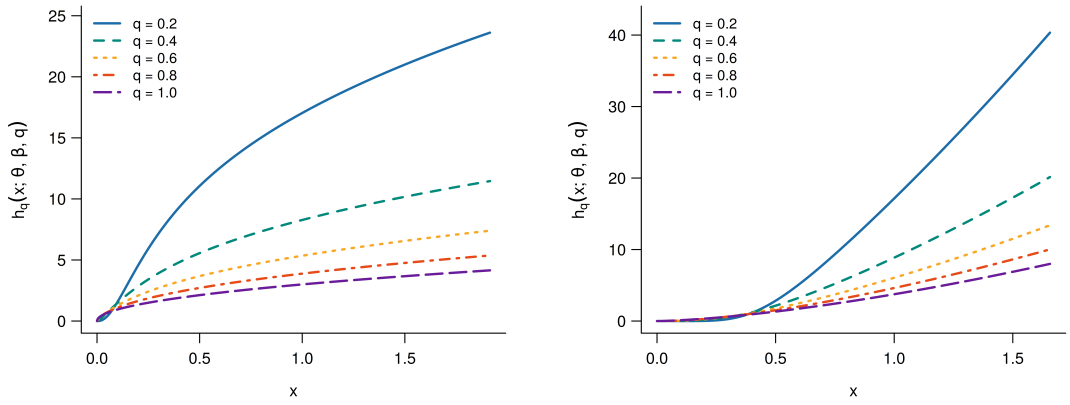
$$S_q(x) = \frac{f_q(x)}{\varphi'(x)}[1 + O(x^{-\theta})].$$

Consequently,

$$h_q(x) = \varphi'(x)\left[1 + O(x^{-\theta})\right] = \frac{\beta\theta}{q} x^{\theta-1} + \frac{1-q}{q} + O(x^{-1}),$$

which also implies that $h_q(x) \to \infty$ as $x \to \infty$.
(iv) Immediate from (ii) and the standard chain of aging implications, IFR $\Rightarrow$ IFRA $\Rightarrow$ NBU $\Rightarrow$ NBUE, together with IFR $\Rightarrow$ DMRL. Strict log-concavity, together with $f_q(0^+) = 0$ and $f_q(x) \to 0$ as $x \to \infty$, implies that the density has a unique mode and is strictly unimodal. □

Proposition 2.1 establishes analytically that the hazard function of the UDFWD increases strictly over the parameter space under consideration. Figure 3 makes the same point graphically: Every curve rises from $h_q(0^+) = 0$, and the smaller q becomes, the higher and steeper the resulting hazard, exactly as the asymptotic expansion in part (iii) predicts. In lifetime terms, the conditional tendency to fail increases as the lifetime progresses. In reliability applications, this behavior can be associated with aging or with the accumulation of deterioration over time. Strict log-concavity guarantees a unique mode of the distribution, and additional structural support is provided for the IFR property, which has been established analytically. The interpretation of a lifetime model suited to the data thus becomes clearer and more straightforward.



(a) $\theta = 1.5, \beta = 2$. **(b)** $\theta = 2.5, \beta = 1.5$.

Figure 3. Hazard-function curves of the UDFWD for selected values of q.

Part (iii) of Proposition 2.1 gives

$$h_q(x) \sim \frac{\beta\theta}{q}\, x^{\theta-1} \quad \text{as} \quad x \to \infty.$$

Write $h_W(x) = \beta\theta x^{\theta-1}$ for the hazard rate function of the WD; then,

$$\lim_{x\to\infty} \frac{h_q(x)}{h_W(x)} = \frac{1}{q}.$$

In the right tail, the hazard rate of the UDFWD is approximately $1/q$ times that of the classical WD, a ratio that grows as q decreases. The constant $(1-q)/q$ in the same expansion does not depend on x and is strictly positive for $0 < q < 1$, so it shifts the hazard rate upward by a fixed amount at large x. In reliability applications, this allows the model to represent systems whose aging or deterioration is more pronounced, while in biomedical survival analysis, where x is the time to an event, the same mechanism corresponds to an event intensity that increases more rapidly with time. Within the parameter space studied analytically, then, the flexibility introduced by q concerns the level and growth of an increasing hazard rate, not transitions among decreasing, bathtub, or unimodal hazard-rate classes.

3. Statistical properties of the UDFWD

This section presents some important statistical properties of the UDFWD. In particular, the mode, quantile function, moments, and entropy measures are derived and discussed.

3.1. Mode of the UDFWD

For $X \sim \text{UDFWD}(\theta, \beta, q)$, the mode is the value at which the PDF in Eq (2.4) attains its maximum. Because the normalizing factor is positive and does not depend on x, it is sufficient to differentiate the x-dependent part of the density. Thus,

$$\frac{d}{dx}\left[x^{\frac{\theta-1}{q}} e^{-\frac{1-q}{q}x-\frac{\beta}{q}x^{\theta}}\right] = x^{\frac{\theta-1}{q}-1} e^{-\frac{1-q}{q}x-\frac{\beta}{q}x^{\theta}}\left[\frac{\theta-1}{q} - \frac{1-q}{q}x - \frac{\beta\theta}{q}x^{\theta}\right].$$

Therefore, the mode x_{mode} is the positive solution of

$$\beta\theta x_{\text{mode}}^{\theta} + (1-q)x_{\text{mode}} = \theta - 1. \tag{3.1}$$

Under $\theta > 1$, $\beta > 0$, and $0 < q \leq 1$, Eq (3.1) has a unique positive solution, as its left-hand side is strictly increasing from zero to infinity. Hence, x_{mode} is the unique mode of the UDFWD and is characterized by the unique positive solution of Eq (3.1).

Moreover, when $q \to 1^-$, Eq (3.1) reduces to the mode of the classical WD:

$$x_{\text{mode}} = \left(\frac{\theta-1}{\beta\theta}\right)^{\frac{1}{\theta}}, \qquad \theta > 1.$$

3.2. Quantile function of the UDFWD

For $X \sim \text{UDFWD}(\theta, \beta, q)$, the quantile function is useful for obtaining the median and other lifetime percentiles. It is also used to generate random observations from the proposed distribution. Let $0 < p < 1$. The pth quantile, denoted by x_p, satisfies

$$F_q(x_p; \theta, \beta, q) = p.$$

Using the CDF in Eq (2.5), x_p is the positive root of

$$\sum_{j=0}^{\infty} \frac{\left[-\frac{1-q}{q}\left(\frac{\beta}{q}\right)^{-\frac{1}{\theta}}\right]^j}{j!} \gamma\left(\frac{\theta + q(j+1) - 1}{q\theta}, \frac{\beta}{q} x_p^{\theta}\right) - p \sum_{j=0}^{\infty} \frac{\left[-\frac{1-q}{q}\left(\frac{\beta}{q}\right)^{-\frac{1}{\theta}}\right]^j}{j!} \Gamma\left(\frac{\theta + q(j+1) - 1}{q\theta}\right) = 0. \tag{3.2}$$

Because Eq (3.2) does not have an explicit solution, x_p is obtained numerically by inversion of the CDF.

For random variate generation, let $U \sim \text{Uniform}(0, 1)$. Then, a random observation from the UDFWD is generated by

$$X = F_q^{-1}(U).$$

Moreover, when $q \to 1^-$, the quantile function of the classical WD is recovered as

$$x_p = \left[\frac{-\log(1-p)}{\beta}\right]^{\frac{1}{\theta}}, \qquad 0 < p < 1.$$

3.3. Moments of the UDFWD

Moments are useful numerical measures for describing the central tendency, variability, skewness, and kurtosis of a probability distribution. They also provide important information about lifetime and reliability data.

Theorem 3.1. *Let $X \sim \text{UDFWD}(\theta, \beta, q)$. Then, for $r = 1, 2, 3, \ldots$, the rth ordinary moment of X is given by*

$$E(X^r) = \left(\frac{\beta}{q}\right)^{-\frac{r}{\theta}} \frac{\displaystyle\sum_{j=0}^{\infty} \frac{\left[-\frac{1-q}{q}\left(\frac{\beta}{q}\right)^{-\frac{1}{\theta}}\right]^j}{j!} \Gamma\left(\frac{\theta + q(r+j+1) - 1}{q\theta}\right)}{\displaystyle\sum_{j=0}^{\infty} \frac{\left[-\frac{1-q}{q}\left(\frac{\beta}{q}\right)^{-\frac{1}{\theta}}\right]^j}{j!} \Gamma\left(\frac{\theta + q(j+1) - 1}{q\theta}\right)}. \tag{3.3}$$

Proof. By definition, the rth ordinary moment is

$$E(X^r) = \int_0^{\infty} x^r f_q(x; \theta, \beta, q)\, dx.$$

Substituting the PDF in Eq (2.4), using the series expansion

$$e^{-\frac{1-q}{q}x} = \sum_{j=0}^{\infty} \frac{\left(-\frac{1-q}{q}x\right)^j}{j!},$$

and interchanging the order of summation and integration gives

$$E(X^r) = \frac{\theta\left(\frac{\beta}{q}\right)^{\frac{\theta+q-1}{q\theta}}}{\sum_{j=0}^{\infty} \frac{\left[-\frac{1-q}{q}\left(\frac{\beta}{q}\right)^{-\frac{1}{\theta}}\right]^j}{j!}\Gamma\left(\frac{\theta+q(j+1)-1}{q\theta}\right)} \times \sum_{j=0}^{\infty} \frac{\left(-\frac{1-q}{q}\right)^j}{j!} \int_0^{\infty} x^{r+\frac{\theta-1}{q}+j} e^{-\frac{\beta}{q}x^{\theta}}\, dx.$$

Using the substitution

$$u = \frac{\beta}{q}x^{\theta},$$

the integral becomes

$$\int_0^{\infty} x^{r+\frac{\theta-1}{q}+j} e^{-\frac{\beta}{q}x^{\theta}}\, dx = \frac{1}{\theta}\left(\frac{\beta}{q}\right)^{-\frac{\theta+q(r+j+1)-1}{q\theta}} \Gamma\left(\frac{\theta+q(r+j+1)-1}{q\theta}\right).$$

Substituting the preceding result and simplifying the powers of β/q give Eq (3.3). □

By taking $r = 1$ in Eq (3.3), the mean of $X \sim \text{UDFWD}(\theta, \beta, q)$ is given by

$$E(X) = \left(\frac{\beta}{q}\right)^{-\frac{1}{\theta}} \frac{\sum_{j=0}^{\infty} \frac{\left[-\frac{1-q}{q}\left(\frac{\beta}{q}\right)^{-\frac{1}{\theta}}\right]^j}{j!}\Gamma\left(\frac{\theta+q(j+2)-1}{q\theta}\right)}{\sum_{j=0}^{\infty} \frac{\left[-\frac{1-q}{q}\left(\frac{\beta}{q}\right)^{-\frac{1}{\theta}}\right]^j}{j!}\Gamma\left(\frac{\theta+q(j+1)-1}{q\theta}\right)}. \tag{3.4}$$

Similarly, by taking $r = 2, 3$, and 4 in Eq (3.3), the remaining ordinary moments required to obtain the variance, skewness, and kurtosis are obtained. Therefore,

$$\text{Var}(X) = E(X^2) - [E(X)]^2,$$

$$\gamma_1 = \frac{E(X^3) - 3E(X)E(X^2) + 2[E(X)]^3}{\{E(X^2) - [E(X)]^2\}^{\frac{3}{2}}},$$

$$\gamma_2 = \frac{E(X^4) - 4E(X)E(X^3) + 6[E(X)]^2E(X^2) - 3[E(X)]^4}{\{E(X^2) - [E(X)]^2\}^2}.$$

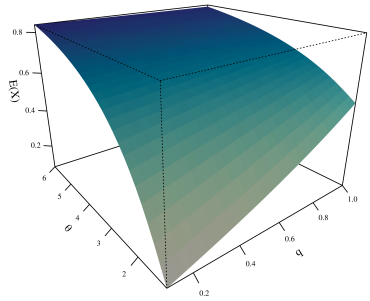
Moreover, when $q \to 1^-$, only the term corresponding to $j = 0$ remains in Eq (3.3). Hence,

$$\lim_{q\to 1^-} E(X^r) = \beta^{-\frac{r}{\theta}}\Gamma\left(1 + \frac{r}{\theta}\right),$$

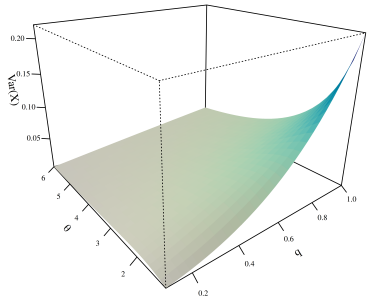
which is the rth ordinary moment of the classical WD.

The combined effects of θ and q on the main numerical characteristics of the UDFWD are illustrated in Figure 4, with $\beta = 2$. The surfaces show that the variance increases with q, whereas the skewness

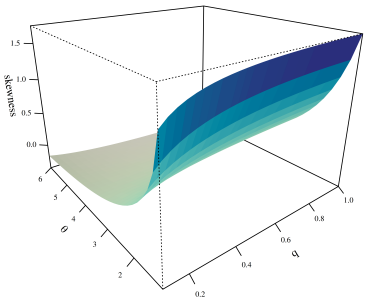
and the kurtosis are governed mainly by θ; the skewness changes sign as θ increases, so that the model can represent right-skewed, nearly symmetric, and slightly left-skewed shapes.



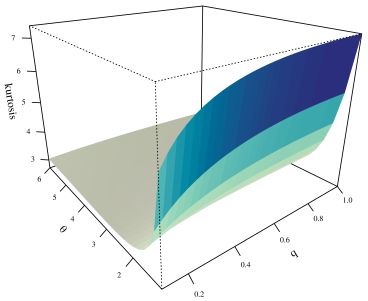
(a) Mean, $\beta = 2$.



(b) Variance, $\beta = 2$.



(c) Skewness, $\beta = 2$.



(d) Kurtosis, $\beta = 2$.

Figure 4. Effects of θ and q on the moment-based measures of the UDFWD for $\beta = 2$.

3.4. Entropy measures of the UDFWD

Entropy measures are useful for describing the uncertainty, randomness, and information content of a probability distribution. In lifetime and reliability analysis, they can be used to compare the uncertainty associated with different failure-time models. In this subsection, the Shannon, Tsallis, and Rényi entropies of the UDFWD are derived.

3.4.1. Shannon entropy of the UDFWD

For $X \sim \text{UDFWD}(\theta, \beta, q)$, the Shannon entropy is defined by:

$$H(X) = -E[\log f_q(X; \theta, \beta, q)].$$

Using the PDF in Eq (2.4), with the normalizing constant C given in Eq (2.3), it follows that:

$$\log f_q(x; \theta, \beta, q) = \log C + \frac{\theta - 1}{q} \log x - \frac{1 - q}{q} x - \frac{\beta}{q} x^{\theta}.$$

Therefore, the Shannon entropy can be written as:

$$H(X) = -\log C - \frac{\theta - 1}{q} E(\log X) + \frac{1 - q}{q} E(X) + \frac{\beta}{q} E(X^{\theta}). \tag{3.5}$$

The mean $E(X)$ is given in Eq (3.4). Also, by taking $r = \theta$ in Eq (3.3), it follows that:

$$E(X^{\theta}) = \Big(\frac{\beta}{q}\Big)^{-1} \frac{\displaystyle\sum_{j=0}^{\infty} \frac{\Big[-\frac{1-q}{q}\big(\frac{\beta}{q}\big)^{-\frac{1}{\theta}}\Big]^{j}}{j!}\Gamma\Big(\frac{\theta + q(\theta + j + 1) - 1}{q\theta}\Big)}{\displaystyle\sum_{j=0}^{\infty} \frac{\Big[-\frac{1-q}{q}\big(\frac{\beta}{q}\big)^{-\frac{1}{\theta}}\Big]^{j}}{j!}\Gamma\Big(\frac{\theta + q(j + 1) - 1}{q\theta}\Big)}. \tag{3.6}$$

It remains to obtain $E(\log X)$. By definition,

$$E(\log X) = \int_0^{\infty} \log x \, f_q(x; \theta, \beta, q)\, dx.$$

Substituting the density and using the series expansion

$$e^{-\frac{1-q}{q}x} = \sum_{j=0}^{\infty} \frac{(-\frac{1-q}{q}x)^{j}}{j!},$$

gives

$$E(\log X) = C \sum_{j=0}^{\infty} \frac{(-\frac{1-q}{q})^{j}}{j!} \int_0^{\infty} x^{\frac{\theta-1}{q}+j} \log x \, e^{-\frac{\beta}{q}x^{\theta}}\, dx,$$

where the order of summation and integration is interchanged under the absolute convergence condition. Using the substitution

$$u = \frac{\beta}{q}x^{\theta},$$

the integral becomes:

$$\int_0^{\infty} x^{\frac{\theta-1}{q}+j} \log x \, e^{-\frac{\beta}{q}x^{\theta}}\, dx = \frac{1}{\theta^2}\Big(\frac{\beta}{q}\Big)^{-\frac{\theta+q(j+1)-1}{q\theta}} \Gamma\Big(\frac{\theta + q(j+1) - 1}{q\theta}\Big)\Big[\psi\Big(\frac{\theta + q(j+1) - 1}{q\theta}\Big) - \log\Big(\frac{\beta}{q}\Big)\Big],$$

where $\psi(\cdot)$ is the digamma function. Substituting the preceding result and using Eq (2.3) gives

$$E(\log X) = \frac{1}{\theta} \frac{\displaystyle\sum_{j=0}^{\infty} \frac{\Big[-\frac{1-q}{q}\big(\frac{\beta}{q}\big)^{-\frac{1}{\theta}}\Big]^{j}}{j!}\Gamma\Big(\frac{\theta + q(j+1) - 1}{q\theta}\Big)\Big[\psi\Big(\frac{\theta + q(j+1) - 1}{q\theta}\Big) - \log\big(\frac{\beta}{q}\big)\Big]}{\displaystyle\sum_{j=0}^{\infty} \frac{\Big[-\frac{1-q}{q}\big(\frac{\beta}{q}\big)^{-\frac{1}{\theta}}\Big]^{j}}{j!}\Gamma\Big(\frac{\theta + q(j+1) - 1}{q\theta}\Big)}. \tag{3.7}$$

Consequently, substituting Eqs (3.4), (3.6), and (3.7) into Eq (3.5) gives the Shannon entropy of the UDFWD.

3.4.2. Tsallis Entropy of the UDFWD

For $X \sim \text{UDFWD}(\theta, \beta, q)$ and $\delta > 0$, $\delta \neq 1$, the Tsallis entropy is defined by

$$T_\delta(X) = \frac{1}{\delta - 1}\left[1 - \int_0^\infty f_q^\delta(x; \theta, \beta, q)\, dx\right].$$

Using the density in Eq (2.4), the required integral can be written as

$$\int_0^\infty f_q^\delta(x; \theta, \beta, q)\, dx = C^\delta \int_0^\infty x^{\frac{\delta(\theta-1)}{q}} e^{-\frac{\delta(1-q)}{q}x - \frac{\delta\beta}{q}x^\theta}\, dx.$$

Using the series expansion

$$e^{-\frac{\delta(1-q)}{q}x} = \sum_{j=0}^{\infty} \frac{(-\frac{\delta(1-q)}{q}x)^j}{j!},$$

and interchanging the order of summation and integration gives

$$\int_0^\infty f_q^\delta(x; \theta, \beta, q)\, dx = C^\delta \sum_{j=0}^{\infty} \frac{(-\frac{\delta(1-q)}{q})^j}{j!} \int_0^\infty x^{\frac{\delta(\theta-1)}{q}+j} e^{-\frac{\delta\beta}{q}x^\theta}\, dx.$$

Using the substitution

$$u = \frac{\delta\beta}{q}x^\theta,$$

the integral becomes

$$\int_0^\infty x^{\frac{\delta(\theta-1)}{q}+j} e^{-\frac{\delta\beta}{q}x^\theta}\, dx = \frac{1}{\theta}\Big(\frac{\delta\beta}{q}\Big)^{-\frac{\delta(\theta-1)+q(j+1)}{q\theta}} \Gamma\Big(\frac{\delta(\theta-1)+q(j+1)}{q\theta}\Big).$$

Therefore,

$$\int_0^\infty f_q^\delta(x; \theta, \beta, q)\, dx = \frac{C^\delta}{\theta} \sum_{j=0}^{\infty} \frac{(-\frac{\delta(1-q)}{q})^j}{j!}\Big(\frac{\delta\beta}{q}\Big)^{-\frac{\delta(\theta-1)+q(j+1)}{q\theta}} \Gamma\Big(\frac{\delta(\theta-1)+q(j+1)}{q\theta}\Big). \tag{3.8}$$

Hence, the Tsallis entropy of the UDFWD is given by

$$T_\delta(X) = \frac{1}{\delta - 1}\Bigg[1 - \frac{C^\delta}{\theta} \sum_{j=0}^{\infty} \frac{(-\frac{\delta(1-q)}{q})^j}{j!}\Big(\frac{\delta\beta}{q}\Big)^{-\frac{\delta(\theta-1)+q(j+1)}{q\theta}} \Gamma\Big(\frac{\delta(\theta-1)+q(j+1)}{q\theta}\Big)\Bigg]. \tag{3.9}$$

This result holds for $\delta > 0$, $\delta \neq 1$, $\theta > 1$, $\beta > 0$, and $0 < q \leq 1$. Moreover, by applying L'Hôpital's rule, the Shannon entropy is recovered as the limiting case of the Tsallis entropy when $\delta \to 1$.

3.4.3. Rényi Entropy of the UDFWD

For $X \sim \text{UDFWD}(\theta, \beta, q)$ and $\delta > 0$, $\delta \neq 1$, the Rényi entropy is defined by

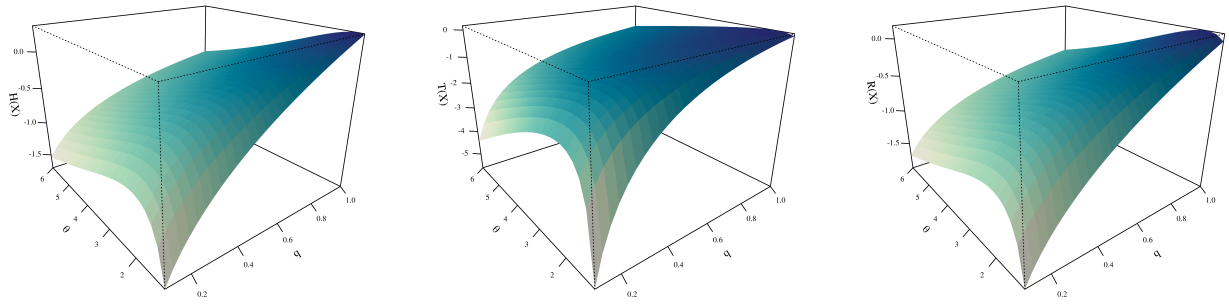
$$R_\delta(X) = \frac{1}{1 - \delta} \log\left[\int_0^\infty f_q^\delta(x; \theta, \beta, q)\, dx\right].$$

Using Eq (3.8), the Rényi entropy of the UDFWD is given by

$$R_\delta(X) = \frac{1}{1-\delta}\log\left[\frac{C^\delta}{\theta}\sum_{j=0}^{\infty}\frac{(-\frac{\delta(1-q)}{q})^j}{j!}\Big(\frac{\delta\beta}{q}\Big)^{-\frac{\delta(\theta-1)+q(j+1)}{q\theta}}\Gamma\Big(\frac{\delta(\theta-1)+q(j+1)}{q\theta}\Big)\right]. \tag{3.10}$$

This result holds for $\delta > 0$, $\delta \neq 1$, $\theta > 1$, $\beta > 0$, and $0 < q \leq 1$. The absolute convergence of the series appearing in Eqs (3.9) and (3.10) is established in Appendix B.

Figure 5 illustrates the effects of θ and q on the entropy measures of the UDFWD. The three surfaces increase steadily with q, indicating that small values of q correspond to a highly concentrated distribution with low uncertainty. In contrast, values close to one correspond to a more dispersed distribution.



(a) Shannon, $\beta = 2$. **(b)** Tsallis, $\delta = 2, \beta = 2$. **(c)** Rényi, $\delta = 2, \beta = 2$.

Figure 5. Effects of θ and q on the entropy measures of the UDFWD for $\beta = 2$.

For the numerical evaluations in Sections 2 and 3, the corresponding integrals were evaluated directly after the transformation $x = e^s$, rather than by truncating the infinite-series representations.

3.5. Stochastic ordering of the UDFWD

Stochastic ordering provides a useful way to compare two lifetime distributions without relying on a single numerical characteristic. Let $X_r \sim \text{UDFWD}(\theta, \beta_r, q)$; $r = 1, 2$ with $\theta > 1$; $0 < q \leq 1$; and $\beta_2 > \beta_1 > 0$. Denote the corresponding normalizing constants by C_1 and C_2. From Eq (2.1),

$$\frac{f_q(x;\theta,\beta_2,q)}{f_q(x;\theta,\beta_1,q)} = \frac{C_2}{C_1}e^{-\frac{\beta_2-\beta_1}{q}x^\theta}.$$

Hence,

$$\frac{d}{dx}\log\frac{f_q(x;\theta,\beta_2,q)}{f_q(x;\theta,\beta_1,q)} = -\frac{\theta(\beta_2-\beta_1)}{q}x^{\theta-1} < 0, \qquad x > 0.$$

Therefore, the density ratio is strictly decreasing in x, and

$$X_2 \leq_{\text{lr}} X_1,$$

where $\leq_{\text{lr}}$ denotes the likelihood-ratio order. The standard implications among stochastic orders then give

$$X_2 \leq_{\text{hr}} X_1 \quad \Longrightarrow \quad X_2 \leq_{\text{st}} X_1,$$

where $\leq_{\text{hr}}$ and $\leq_{\text{st}}$ denote the hazard-rate and usual stochastic orders, respectively. Thus, for fixed θ and q, increasing β shifts the UDFWD toward smaller values. Under a lifetime interpretation, this corresponds to shorter lifetimes and a greater failure tendency.

The fractional parameter has a different effect. For fixed θ and β, let $0 < q_1 < q_2 \leq 1$. Then,

$$\frac{d}{dx}\log\frac{f_{q_2}(x;\theta,\beta,q_2)}{f_{q_1}(x;\theta,\beta,q_1)} = \left(\frac{1}{q_2}-\frac{1}{q_1}\right)\left[\frac{\theta-1}{x}-1-\beta\theta\,x^{\theta-1}\right].$$

Define

$$B(x) = \frac{\theta-1}{x}-1-\beta\theta\,x^{\theta-1}.$$

For $\theta > 1$,

$$B'(x) = -\frac{\theta-1}{x^2}-\beta\theta(\theta-1)\,x^{\theta-2} < 0, \qquad x > 0,$$

and

$$\lim_{x\to 0^+} B(x) = +\infty, \qquad \lim_{x\to\infty} B(x) = -\infty.$$

Hence, $B(x)$ changes sign exactly once. Because

$$\frac{1}{q_2}-\frac{1}{q_1} < 0,$$

the derivative of the log-density ratio also changes sign once. Therefore,

$$\frac{f_q(x;\theta,\beta,q_2)}{f_q(x;\theta,\beta,q_1)}$$

is strictly decreasing on $(0, x_0)$ and strictly increasing on (x_0, ∞), where x_0 is the unique zero of $B(x)$. The density ratio is not monotone, so q doesn't induce a global likelihood-ratio ordering over the whole parameter space.

4. Parameter estimation and simulation

This section addresses parameter estimation for the proposed model, followed by a Monte Carlo simulation study to assess the performance of the resulting estimators numerically.

4.1. Parameter estimation

Here, the parameters of the UDFWD are estimated using maximum likelihood, least squares, and weighted least squares. For estimation of the three-parameter UDFWD, the parameter space is restricted to $\theta > 1, \beta > 0$, and $0 < q < 1$. The endpoint $q = 1$ corresponds exactly to the classical WD and is therefore treated as the classical boundary case rather than as an estimable fractional value.

4.1.1. Maximum likelihood estimation

Let $X_1, X_2, \ldots, X_n \overset{\text{i.i.d.}}{\sim} \text{UDFWD}(\theta, \beta, q)$ with corresponding observed values $x_1, x_2, \ldots, x_n$. Then, the likelihood function for (θ, β, q) is given by

$$L(\theta,\beta,q) = \prod_{i=1}^{n} f_q(x_i;\theta,\beta,q) = \frac{\theta^n \left(\frac{\beta}{q}\right)^{\frac{n(\theta+q-1)}{q\theta}} \prod_{i=1}^{n} x_i^{\frac{\theta-1}{q}} e^{\left[-\frac{1-q}{q}\sum_{i=1}^{n} x_i - \frac{\beta}{q}\sum_{i=1}^{n} x_i^{\theta}\right]}}{\left[\sum_{j=0}^{\infty} \frac{\left[-\frac{1-q}{q}\left(\frac{\beta}{q}\right)^{-\frac{1}{\theta}}\right]^j}{j!}\Gamma\left(\frac{\theta+q(j+1)-1}{q\theta}\right)\right]^n}. \tag{4.1}$$

The log-likelihood function is

$$\begin{aligned}\ell(\theta,\beta,q) = {} & n\log\theta + \frac{n(\theta+q-1)}{q\theta}\log\left(\frac{\beta}{q}\right) + \frac{\theta-1}{q}\sum_{i=1}^{n}\log x_i \\ & - \frac{1-q}{q}\sum_{i=1}^{n} x_i - \frac{\beta}{q}\sum_{i=1}^{n} x_i^{\theta} \\ & - n\log\left[\sum_{j=0}^{\infty} \frac{\left[-\frac{1-q}{q}\left(\frac{\beta}{q}\right)^{-\frac{1}{\theta}}\right]^j}{j!}\Gamma\left(\frac{\theta+q(j+1)-1}{q\theta}\right)\right].\end{aligned} \tag{4.2}$$

The maximum likelihood estimates (MLEs) of θ, β, and q, denoted $\hat{\theta}_{\text{MLE}}$, $\hat{\beta}_{\text{MLE}}$, and $\hat{q}_{\text{MLE}}$, respectively, are obtained by differentiating the log-likelihood function partially with respect to each parameter and setting the resulting derivatives equal to zero. This yields the likelihood equations, given as follows:

$$\begin{aligned}\frac{\partial\ell(\theta,\beta,q)}{\partial\theta} = {} & \frac{n}{\theta} + \frac{n(1-q)}{q\theta^2}\log\left(\frac{\beta}{q}\right) + \frac{1}{q}\sum_{i=1}^{n}\log x_i - \frac{\beta}{q}\sum_{i=1}^{n} x_i^{\theta}\log x_i \\ & - \frac{n\sum_{j=0}^{\infty} \frac{\left[-\frac{1-q}{q}\left(\frac{\beta}{q}\right)^{-\frac{1}{\theta}}\right]^j}{j!}\Gamma\left(\frac{\theta+q(j+1)-1}{q\theta}\right) \times \left[\frac{j}{\theta^2}\log\left(\frac{\beta}{q}\right) + \frac{1-q(j+1)}{q\theta^2}\psi\left(\frac{\theta+q(j+1)-1}{q\theta}\right)\right]}{\sum_{j=0}^{\infty} \frac{\left[-\frac{1-q}{q}\left(\frac{\beta}{q}\right)^{-\frac{1}{\theta}}\right]^j}{j!}\Gamma\left(\frac{\theta+q(j+1)-1}{q\theta}\right)} = 0,\end{aligned} \tag{4.3}$$

where $\psi(\cdot)$ is the digamma function,

$$\frac{\partial \ell(\theta,\beta,q)}{\partial \beta} = \frac{n(\theta+q-1)}{q\theta\beta} - \frac{1}{q}\sum_{i=1}^{n} x_i^{\theta} + \frac{n\sum_{j=0}^{\infty} \frac{j\left[-\frac{1-q}{q}\left(\frac{\beta}{q}\right)^{-\frac{1}{\theta}}\right]^{j}}{\theta\beta j!}\Gamma\left(\frac{\theta+q(j+1)-1}{q\theta}\right)}{\sum_{j=0}^{\infty} \frac{\left[-\frac{1-q}{q}\left(\frac{\beta}{q}\right)^{-\frac{1}{\theta}}\right]^{j}}{j!}\Gamma\left(\frac{\theta+q(j+1)-1}{q\theta}\right)} = 0, \tag{4.4}$$

and

$$\begin{aligned}\frac{\partial \ell(\theta,\beta,q)}{\partial q} = &-\frac{n(\theta+q-1)}{q^2\theta} - \frac{n(\theta-1)}{q^2\theta}\log\left(\frac{\beta}{q}\right) - \frac{\theta-1}{q^2}\sum_{i=1}^{n}\log x_i \\ &+ \frac{1}{q^2}\sum_{i=1}^{n} x_i + \frac{\beta}{q^2}\sum_{i=1}^{n} x_i^{\theta} - \frac{n\sum_{j=0}^{\infty} \frac{\left[-\frac{1-q}{q}\left(\frac{\beta}{q}\right)^{-\frac{1}{\theta}}\right]^{j}}{j!}\Gamma\left(\frac{\theta+q(j+1)-1}{q\theta}\right) \times \left[j\left(-\frac{1}{1-q}-\frac{1}{q}+\frac{1}{\theta q}\right) - \frac{\theta-1}{q^2\theta}\psi\left(\frac{\theta+q(j+1)-1}{q\theta}\right)\right]}{\sum_{j=0}^{\infty} \frac{\left[-\frac{1-q}{q}\left(\frac{\beta}{q}\right)^{-\frac{1}{\theta}}\right]^{j}}{j!}\Gamma\left(\frac{\theta+q(j+1)-1}{q\theta}\right)} = 0.\end{aligned} \tag{4.5}$$

Because the preceding nonlinear equations do not admit explicit closed-form solutions, the MLEs are obtained numerically by maximizing the log-likelihood function over the parameter space $\theta > 1, \beta > 0$, and $0 < q < 1$.

In the numerical maximization, the infinite series is not truncated. Instead, the normalizing constant is evaluated from its integral representation by adaptive quadrature, with absolute and relative tolerances set to 10^{-8}, which improves numerical stability. Optimization is carried out under the parameter constraints, with exponential reparameterizations used to enforce $\theta > 1$ and $\beta > 0$, and q is restricted to the admissible interval $0 < q < 1$. Several starting values are used to reduce sensitivity to initialization.

4.1.2. Least squares estimation

Let $X_{(1)} \le X_{(2)} \le \cdots \le X_{(n)}$ be the order statistics of a random sample of size n from UDFWD(θ,β,q). The least-squares estimation (LSE) method is based on fitting the theoretical CDF to the empirical plotting positions. For a continuous distribution,

$$E\left[F_q\left(X_{(i)};\theta,\beta,q\right)\right] = \frac{i}{n+1}, \qquad i = 1,2,\ldots,n.$$

Therefore, the least-squares objective function is defined by

$$Q(\theta,\beta,q) = \sum_{i=1}^{n}\left[F_q\left(x_{(i)};\theta,\beta,q\right) - \frac{i}{n+1}\right]^2. \tag{4.6}$$

The LSEs of θ, β, and q are given by

$$(\hat{\theta}_{\text{LSE}}, \hat{\beta}_{\text{LSE}}, \hat{q}_{\text{LSE}}) = \underset{\theta>1, \beta>0, 0<q<1}{\arg\min} \; Q(\theta, \beta, q).$$

Substituting the CDF in Eq (2.5) into Eq (4.6), the least squares objective function becomes:

$$Q(\theta,\beta,q) = \sum_{i=1}^{n}\left[\frac{\sum_{j=0}^{\infty}\frac{\left[-\frac{1-q}{q}\left(\frac{\beta}{q}\right)^{-\frac{1}{\theta}}\right]^{j}}{j!}\gamma\left(\frac{\theta+q(j+1)-1}{q\theta}, \frac{\beta}{q}x_{(i)}^{\theta}\right)}{\sum_{j=0}^{\infty}\frac{\left[-\frac{1-q}{q}\left(\frac{\beta}{q}\right)^{-\frac{1}{\theta}}\right]^{j}}{j!}\Gamma\left(\frac{\theta+q(j+1)-1}{q\theta}\right)} - \frac{i}{n+1}\right]^{2}.$$

Thus, the LSEs satisfy the following nonlinear estimating equations:

$$\frac{\partial Q(\theta,\beta,q)}{\partial\theta} = 0, \qquad \frac{\partial Q(\theta,\beta,q)}{\partial\beta} = 0, \qquad \frac{\partial Q(\theta,\beta,q)}{\partial q} = 0.$$

Because these nonlinear equations involve infinite series and incomplete gamma functions, they do not admit explicit closed-form solutions. Therefore, the LSEs are obtained numerically.

4.1.3. Weighted least squares estimation

The weights used in the weighted least-squares estimation method are defined by

$$W_i = \frac{(n+1)^2(n+2)}{i(n-i+1)}, \qquad i = 1, 2, \ldots, n.$$

The WLSEs of θ, β, and q are obtained by minimizing the weighted least squares objective function defined by

$$WL(\theta,\beta,q) = \sum_{i=1}^{n} W_i\left[F_q\left(x_{(i)};\theta,\beta,q\right) - \frac{i}{n+1}\right]^{2}. \tag{4.7}$$

Thus,

$$(\hat{\theta}_{\text{WLSE}}, \hat{\beta}_{\text{WLSE}}, \hat{q}_{\text{WLSE}}) = \underset{\theta>1, \beta>0, 0<q<1}{\arg\min} \; WL(\theta, \beta, q).$$

Substituting the CDF in Eq (2.5) into Eq (4.7), the weighted least-squares objective function becomes

$$WL(\theta,\beta,q) = \sum_{i=1}^{n} W_i\left[\frac{\sum_{j=0}^{\infty}\frac{\left[-\frac{1-q}{q}\left(\frac{\beta}{q}\right)^{-\frac{1}{\theta}}\right]^{j}}{j!}\gamma\left(\frac{\theta+q(j+1)-1}{q\theta}, \frac{\beta}{q}x_{(i)}^{\theta}\right)}{\sum_{j=0}^{\infty}\frac{\left[-\frac{1-q}{q}\left(\frac{\beta}{q}\right)^{-\frac{1}{\theta}}\right]^{j}}{j!}\Gamma\left(\frac{\theta+q(j+1)-1}{q\theta}\right)} - \frac{i}{n+1}\right]^{2}.$$

The WLSEs satisfy the following system of nonlinear estimating equations:

$$\frac{\partial WL(\theta,\beta,q)}{\partial\theta} = 2\sum_{i=1}^{n} W_i\left[F_q(x_{(i)};\theta,\beta,q) - \frac{i}{n+1}\right]\frac{\partial F_q(x_{(i)};\theta,\beta,q)}{\partial\theta} = 0,$$

$$\frac{\partial WL(\theta,\beta,q)}{\partial\beta} = 2\sum_{i=1}^{n} W_i\left[F_q(x_{(i)};\theta,\beta,q) - \frac{i}{n+1}\right]\frac{\partial F_q(x_{(i)};\theta,\beta,q)}{\partial\beta} = 0,$$

$$\frac{\partial WL(\theta,\beta,q)}{\partial q} = 2\sum_{i=1}^{n} W_i\left[F_q(x_{(i)};\theta,\beta,q) - \frac{i}{n+1}\right]\frac{\partial F_q(x_{(i)};\theta,\beta,q)}{\partial q} = 0.$$

Because the preceding nonlinear equations involve infinite series, incomplete gamma functions, and their derivatives, they do not admit explicit closed-form solutions. Therefore, the WLSEs are obtained numerically.

Remark 4.1. *Let $\boldsymbol{\eta}_r = (\theta_r,\beta_r,q_r)$, $r = 1,2$, be two admissible parameter vectors, and suppose $f(x;\boldsymbol{\eta}_1) = f(x;\boldsymbol{\eta}_2)$ for all $x > 0$. Then, Eq (2.1) gives*

$$K + (a_1 - a_2)\log x - (b_1 - b_2)x - c_1x^{\theta_1} + c_2x^{\theta_2} = 0,$$

where

$$K = \log\left(\frac{C_1}{C_2}\right), \qquad a_r = \frac{\theta_r - 1}{q_r},$$
$$b_r = \frac{1-q_r}{q_r}, \qquad c_r = \frac{\beta_r}{q_r}.$$

Comparing the dominant powers as $x \to \infty$ yields $\theta_1 = \theta_2$, followed by $c_1 = c_2$. The remaining identity is

$$K + (a_1 - a_2)\log x - (b_1 - b_2)x = 0.$$

Because x dominates $\log x$ as $x \to \infty$, it follows that $b_1 = b_2$. Moreover,

$$b(q) = \frac{1-q}{q}$$

is one-to-one on $(0,1]$. Hence, $q_1 = q_2$, and $c_1 = c_2$ then gives $\beta_1 = \beta_2$. Thus, the UDFWD is identifiable.

At the population level, identifiability gives a unique target for the MLE, LSE, and WLSE criteria.

4.2. Simulation study

In this subsection, a Monte Carlo simulation study is conducted to investigate the finite-sample performance of the estimators of the UDFWD parameters. We assess the accuracy and stability of the MLE, LSE, and WLSE methods for different parameter values and sample sizes.

Three parameter settings are considered, namely $(\theta,\beta,q) = (1.5,1.0,0.30)$, $(2.0,1.5,0.50)$, and $(3.0,2.0,0.70)$. For each setting, we generate random samples of sizes $n = 25,50,90,100$, and 200. The number of Monte Carlo replications is $N = 1000$.

The simulation algorithm is implemented as follows:

(1) Fix θ, β, and q.
(2) Generate $X_1, X_2, \ldots, X_n \overset{\text{i.i.d.}}{\sim}$ UDFWD(θ, β, q) using a numerical inverse transform method. A numerical inversion strategy of this type is discussed in [27]. Let $U_i \sim$ Uniform$(0, 1)$, and

$$X_i = F_q^{-1}(U_i), \qquad i = 1, 2, \ldots, n.$$

(3) From each generated sample, obtain the MLEs, LSEs, and WLSEs of θ, β, and q.
(4) Repeat Steps 2 and 3 $N = 1000$ times.
(5) For each parameter under each estimation method, compute over the N replications the average estimates (AEs), mean squared errors (MSEs), and relative biases (RBs).
(6) Compare the three estimation methods using their MSEs and absolute RBs.

The results obtained for the three parameter settings are reported in Tables 1–3. Each table reports the AEs, MSEs, and RBs of the MLE, LSE, and WLSE methods for θ, β, and q at different sample sizes.

Table 1. AEs, MSEs, and RBs of the MLEs, LSEs, and WLSEs for the UDFWD under $(\theta, \beta, q) = (1.5, 1, 0.3)$.

n	Method	θ			β			q		
		AE	MSE	RB	AE	MSE	RB	AE	MSE	RB
25	MLE	1.6921	0.2337	0.1280	2.1451	6.9575	1.1451	0.5043	0.1996	0.6811
	LSE	1.6348	0.2042	0.0899	2.0542	6.0116	1.0542	0.5518	0.2298	0.8393
	WLSE	1.6372	0.1976	0.0914	2.0322	5.9249	1.0322	0.5366	0.2180	0.7886
50	MLE	1.6061	0.1390	0.0708	1.6547	3.8174	0.6547	0.4410	0.1500	0.4699
	LSE	1.5996	0.1439	0.0664	1.7844	4.2285	0.7844	0.5011	0.1936	0.6702
	WLSE	1.5913	0.1349	0.0609	1.6968	3.9288	0.6968	0.4755	0.1752	0.5851
90	MLE	1.6089	0.0965	0.0726	1.6290	2.5780	0.6290	0.4430	0.1192	0.4767
	LSE	1.6339	0.1125	0.0892	1.9149	3.5254	0.9149	0.5171	0.1677	0.7237
	WLSE	1.6163	0.1015	0.0776	1.7833	3.0687	0.7833	0.4869	0.1469	0.6230
100	MLE	1.5710	0.0912	0.0474	1.4714	2.5257	0.4714	0.4158	0.1179	0.3861
	LSE	1.5748	0.1084	0.0499	1.5978	3.2273	0.5978	0.4589	0.1603	0.5295
	WLSE	1.5632	0.0958	0.0421	1.4949	2.7538	0.4949	0.4330	0.1360	0.4434
200	MLE	1.5367	0.0578	0.0245	1.2738	1.5627	0.2738	0.3728	0.0746	0.2427
	LSE	1.5643	0.0900	0.0428	1.5068	2.6675	0.5068	0.4329	0.1288	0.4432
	WLSE	1.5453	0.0710	0.0302	1.3607	1.9731	0.3607	0.3979	0.0957	0.3262

Table 2. AEs, MSEs, and RBs of the MLEs, LSEs, and WLSEs for the UDFWD under $(\theta, \beta, q) = (2, 1.5, 0.5)$.

n	Method	θ			β			q		
		AE	MSE	RB	AE	MSE	RB	AE	MSE	RB
25	MLE	2.0640	0.3690	0.0320	1.6796	2.4912	0.1197	0.5529	0.1591	0.1058
	LSE	1.9684	0.3384	-0.0158	1.5822	2.3951	0.0548	0.5938	0.1760	0.1877
	WLSE	1.9731	0.3231	-0.0135	1.5887	2.4210	0.0592	0.5843	0.1702	0.1687
50	MLE	2.0477	0.2311	0.0238	1.6151	1.5071	0.0767	0.5585	0.1334	0.1171
	LSE	1.9833	0.2633	-0.0084	1.5188	1.6821	0.0126	0.5711	0.1613	0.1422
	WLSE	1.9962	0.2404	-0.0019	1.5459	1.5802	0.0306	0.5683	0.1477	0.1366
90	MLE	2.0654	0.1645	0.0327	1.6588	1.0739	0.1059	0.5776	0.1153	0.1551
	LSE	2.0345	0.1683	0.0173	1.6622	1.1317	0.1082	0.6042	0.1298	0.2085
	WLSE	2.0370	0.1539	0.0185	1.6570	1.0507	0.1047	0.5950	0.1199	0.1901
100	MLE	2.0292	0.1596	0.0146	1.5848	1.0803	0.0565	0.5506	0.1076	0.1012
	LSE	2.0003	0.2006	0.0001	1.5591	1.3336	0.0394	0.5760	0.1395	0.1520
	WLSE	2.0103	0.1805	0.0052	1.5736	1.2224	0.0491	0.5695	0.1267	0.1390
200	MLE	2.0344	0.1083	0.0172	1.6129	0.7905	0.0752	0.5607	0.0873	0.1215
	LSE	2.0201	0.1490	0.0101	1.6113	1.0860	0.0742	0.5791	0.1179	0.1582
	WLSE	2.0226	0.1255	0.0113	1.6055	0.9246	0.0704	0.5696	0.1015	0.1391

Table 3. AEs, MSEs, and RBs of the MLEs, LSEs, and WLSEs for the UDFWD under $(\theta, \beta, q) = (3, 2, 0.7)$.

n	Method	θ			β			q		
		AE	MSE	RB	AE	MSE	RB	AE	MSE	RB
25	MLE	2.8946	0.8897	-0.0351	1.8147	1.6286	-0.0926	0.6289	0.1632	-0.1015
	LSE	2.6672	1.0406	-0.1109	1.5478	2.0527	-0.2261	0.6076	0.1816	-0.1321
	WLSE	2.7127	0.9281	-0.0958	1.6165	1.7512	-0.1917	0.6257	0.1727	-0.1062
50	MLE	2.8137	0.6097	-0.0621	1.7266	1.1621	-0.1367	0.6057	0.1411	-0.1347
	LSE	2.6650	0.7862	-0.1117	1.5504	1.4702	-0.2248	0.5928	0.1680	-0.1531
	WLSE	2.7124	0.6952	-0.0959	1.6154	1.2990	-0.1923	0.6052	0.1539	-0.1354
90	MLE	2.8895	0.3771	-0.0368	1.8311	0.6826	-0.0845	0.6448	0.1062	-0.0789
	LSE	2.7970	0.5112	-0.0677	1.7184	0.9081	-0.1408	0.6383	0.1315	-0.0881
	WLSE	2.8392	0.4436	-0.0536	1.7728	0.7697	-0.1136	0.6459	0.1159	-0.0773
100	MLE	2.8978	0.3613	-0.0341	1.8718	0.6727	-0.0641	0.6642	0.0991	-0.0512
	LSE	2.7860	0.5601	-0.0713	1.7243	1.0385	-0.1379	0.6425	0.1358	-0.0821
	WLSE	2.8378	0.4498	-0.0541	1.7982	0.8275	-0.1009	0.6571	0.1153	-0.0613
200	MLE	2.9737	0.2061	-0.0088	1.9649	0.3823	-0.0176	0.7013	0.0688	0.0019
	LSE	2.8532	0.3613	-0.0489	1.8050	0.6713	-0.0975	0.6633	0.1033	-0.0525
	WLSE	2.9109	0.2622	-0.0297	1.8861	0.4870	-0.0570	0.6836	0.0831	-0.0235

Tables 1–3 show that the finite-sample performance of the three estimation methods generally improves as the sample size increases. A decrease in both MSEs and absolute RBs is usually observed with increasing n. For small and moderate samples, however, the estimators differ in their performance. Smaller MSEs than those of the MLE are occasionally obtained with the WLSE. At $n = 90$, the WLSE still shows a slight advantage for two parameters under one of the three settings. The pattern changes for larger samples. At $n = 100$ and 200, the lowest MSEs for all three parameters are obtained with the MLE in every setting considered. Thus, among the sample sizes examined, $n = 100$ is the smallest at which the MLE consistently achieves the lowest MSEs across all parameters and settings.

As the sample size increases, a less pronounced reduction in MSE is observed for $\widehat{q}$ than for $\widehat{\theta}$ and $\widehat{\beta}$. According to Table 3, the MSE of the MLE of q decreases from 0.1632 at $n = 25$ to 0.0688 at $n = 200$. Over the same range, the MSEs of $\widehat{\theta}$ and $\widehat{\beta}$ fall to less than one quarter of their initial values. These results suggest that, under the settings considered, the fractional parameter q may be more difficult to estimate in small samples. The model structure may partly explain this behavior. In the PDF, the parameter q appears through terms such as β/q and is also included in the normalizing constant. Such dependence between q and β may affect the accuracy of estimation, particularly for small n. Considerable numerical computation is also required in the estimation procedure. To evaluate the likelihood, adaptive quadrature is used to calculate the normalizing constant, followed by constrained numerical optimization over the three parameters. Introducing q therefore provides additional flexibility, but greater computational effort is required. Nevertheless, the MSE of $\widehat{q}$ decreases as the sample size increases.

To examine the behavior of the model near the Weibull boundary, local diagnostics were computed for $q = 0.80$, 0.90, and 0.99, with $\theta = 2$ and $\beta = 1.5$ held fixed. The Fisher information matrix for a single observation is denoted by $\mathcal{I}(\theta, \beta, q)$ and defined by

$$\mathcal{I}(\theta,\beta,q) = -\mathrm{E}\left[\frac{\partial^2 \log f_q(X;\theta,\beta,q)}{\partial\boldsymbol{\eta}\partial\boldsymbol{\eta}^\top}\right], \qquad \boldsymbol{\eta} = (\theta,\beta,q)^\top,$$

and its entries were evaluated numerically at these parameter values.

For a sample of size n, the corresponding asymptotic covariance matrix is $n^{-1}\mathcal{I}^{-1}(\theta,\beta,q)$. The Kolmogorov distance between the UDFWD and the classical WD was also calculated as

$$D_W = \sup_{x>0} |F_q(x) - F_W(x)|.$$

In addition, we considered the three pairwise asymptotic correlations among $\widehat{\theta}$, $\widehat{\beta}$, and $\widehat{q}$, together with the element $[\mathcal{I}^{-1}(\theta,\beta,q)]_{qq}$. Table 4 reports the numerical results.

Table 4. Near-Weibull diagnostics for $\theta = 2$ and $\beta = 1.5$.

q	D_W	$\rho_{\widehat{\theta},\widehat{\beta}}$	$\rho_{\widehat{\theta},\widehat{q}}$	$\rho_{\widehat{q},\widehat{\beta}}$	$[\mathcal{I}^{-1}]_{qq}$
0.80	0.0662	0.9496	0.9464	0.9918	51.75
0.90	0.0318	0.9365	0.9385	0.9919	65.61
0.99	0.0031	0.9237	0.9313	0.9918	80.03

Table 4 indicates that D_W decreases from 0.0662 to 0.0031 as q approaches one. All three parameter estimates are strongly positively correlated over these settings. The correlations involving $\widehat{\theta}$ range from

0.9237 to 0.9496, whereas that between $\widehat{q}$ and $\widehat{\beta}$ remains the strongest, at about 0.992. Moreover, $[\mathcal{I}^{-1}]_{qq}$ increases from 51.75 to 80.03, indicating lower asymptotic precision for estimating q near the Weibull boundary. The Fisher information matrix remains nonsingular at the three interior points, with its smallest eigenvalue ranging from 0.004292 to 0.004606.

5. Real data applications

The flexibility of the UDFWD in practice is illustrated in this section by means of two real datasets taken from different applied fields. The first dataset comes from engineering reliability and contains tensile strength measurements of carbon fibers. The second one is biomedical and consists of serum creatinine measurements. For the proposed model, the observations are treated as realizations of $X \sim \text{UDFWD}(\theta, \beta, q)$.

The UDFWD is compared with six competing lifetime distributions selected to represent distinct flexible lifetime model construction mechanisms: The modified Kies-Weibull distribution (MKW), Kumaraswamy-Weibull distribution (KwW), Topp-Leone inverse Weibull distribution (TLIW), inverse Weibull distribution (IW), exponentiated exponential-Weibull distribution (EEW), and exponentiated Nadarajah-Haghighi distribution (ENH). The IW serves as an inverse Weibull benchmark. The TLIW and KwW are based on the Topp-Leone and Kumaraswamy mechanisms, respectively, whereas the MKW represents a modification of the Kies–Weibull model. The EEW and ENH are constructed using exponentiation. In contrast, the UDFWD is obtained by introducing the UD fractional derivative at the differential-equation level.

For each fitted model, the unknown parameters are estimated using maximum likelihood. The models are compared using the negative maximized log-likelihood, Akaike information criterion, corrected Akaike information criterion, Bayesian information criterion, consistent Akaike information criterion, Hannan-Quinn information criterion, Kolmogorov-Smirnov statistic, Cramér-von Mises statistic, Anderson-Darling statistic, and the corresponding Kolmogorov-Smirnov p-value. These measures are denoted by $-\ell$, AIC, AICc, BIC, CAIC, HQIC, K-S, W^2, A^2, and p-value, respectively.

Let ℓ denote the maximized log-likelihood value, k the number of estimated parameters, and n the sample size. The information criteria are computed as

$$\begin{aligned} &\text{AIC} = -2\ell + 2k, && \text{AICc} = \text{AIC} + \frac{2k(k+1)}{n-k-1}, \\ &\text{BIC} = -2\ell + k\log(n), && \text{CAIC} = -2\ell + k[\log(n)+1], \\ &\text{HQIC} = -2\ell + 2k\log[\log(n)]. \end{aligned}$$

Smaller values of AIC, AICc, BIC, CAIC, HQIC, K-S, W^2, and A^2 indicate a better fit. Also, the K-S p-value is reported as an additional goodness-of-fit measure. The graphical summaries used below are treated as empirical diagnostics of the observed data. In contrast, the distributional properties of the UDFWD, including the IFR property, are established analytically in Section 2.

5.1. Dataset I: Carbon fiber tensile strength data

This dataset consists of $n = 69$ carbon fiber tensile strength measurements; see [28]. Tensile strength is the maximum stress a material can withstand under tension before it breaks; for this reason, it

is a fundamental quantity in engineering reliability and materials science. Because all observations are positive and continuous, lifetime distributions are candidate models for the data. The data are as follows:

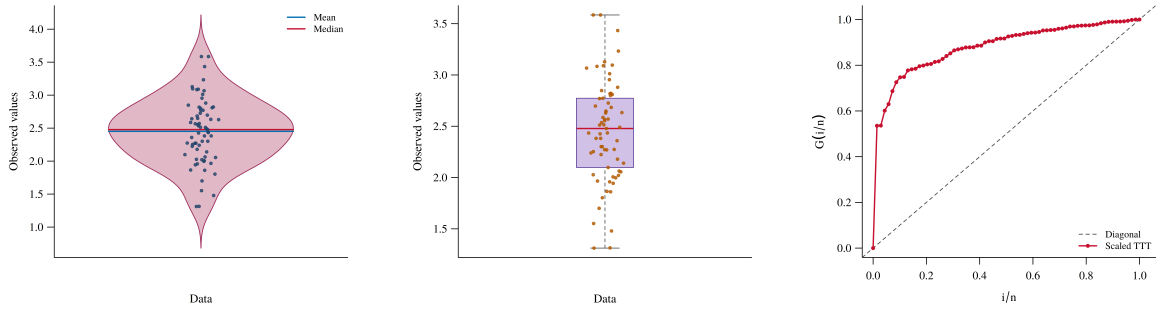
1.312, 1.314, 1.479, 1.552, 1.700, 1.803, 1.861, 1.865, 1.944, 1.958, 1.966, 1.997, 2.006, 2.021, 2.027, 2.055, 2.063, 2.098, 2.140, 2.179, 2.224, 2.240, 2.253, 2.270, 2.272, 2.274, 2.301, 2.301, 2.359, 2.382, 2.382, 2.426, 2.434, 2.435, 2.478, 2.490, 2.511, 2.514, 2.535, 2.554, 2.566, 2.570, 2.586, 2.629, 2.633, 2.642, 2.648, 2.684, 2.697, 2.726, 2.770, 2.773, 2.800, 2.809, 2.818, 2.821, 2.848, 2.880, 2.954, 3.012, 3.067, 3.084, 3.090, 3.096, 3.128, 3.233, 3.433, 3.585, 3.585.

The main descriptive statistics for the 69 measurements are presented in Table 5.

Table 5. Summary statistics for Dataset I.

n	Min.	Q_1.	Median	Mean	Q_3	Max.	SD	Variance	Skewness	Kurtosis
69	1.312	2.098	2.478	2.4513	2.773	3.585	0.4951	0.2452	-0.0288	3.0285

From Table 5, the mean and the median are reported as 2.4513 and 2.478, respectively, and the skewness is −0.0288. Thus, the distribution can be regarded as approximately symmetric. A kurtosis of 3.0285 is also observed, indicating tail behavior close to that of the normal distribution. Figure 6 gives the violin, box, and TTT plots. The TTT curve is concave and lies above the diagonal, which is the typical shape for data with an increasing hazard rate. This behavior is consistent with the IFR property of the fitted UDFWD.



(a) Violin plot. **(b)** Box and strip plot. **(c)** TTT plot.

Figure 6. Exploratory plots for Dataset I.

The MLEs and model selection criteria for Dataset I are reported in Table 6, and the goodness-of-fit statistics are reported in Table 7.

Table 6. MLEs and model selection criteria for Dataset I.

Model	Estimates	$-\ell$	AIC	AICc	BIC	CAIC	HQIC
UDFWD	$\widehat{\theta} = 4.0992$, $\widehat{\beta} = 0.0087$, $\widehat{q} = 0.3255$	48.8807	103.7614	104.1306	110.4637	113.4637	106.4204
ENH	$\widehat{\alpha} = 4.5603 \times 10^{-6}$, $\widehat{\gamma} = 123781.8675$, $\widehat{\lambda} = 12.6601$	49.4403	104.8805	105.2498	111.5828	114.5828	107.5396
MKW	$\widehat{\alpha} = 0.6905$, $\widehat{\beta} = 0.0039$, $\widehat{\gamma} = 1022.6068$	49.5990	105.1980	105.5673	111.9004	114.9004	107.8571
KwW	$\widehat{\delta_1} = 21.6724$, $\widehat{\delta_2} = 92.6822$, $\widehat{\gamma} = 0.8950$, $\widehat{\theta} = 0.6454$	48.8556	105.7112	106.3362	114.6476	118.6476	109.2566
EEW	$\widehat{c} = 3.8633$, $\widehat{\beta} = 3.4671$, $\widehat{\alpha} = 2.0269$, $\widehat{\lambda} = 4.7065$	48.8597	105.7195	106.3445	114.6559	118.6559	109.2649
TLIW	$\widehat{\alpha} = 2.8328$, $\widehat{\beta} = 3.4115$, $\widehat{\lambda} = 0.5468$	58.0304	122.0608	122.4300	128.7631	131.7631	124.7199
IW	$\widehat{\eta} = 4.1267$, $\widehat{\gamma} = 23.2618$	63.6236	131.2472	131.4290	135.7154	137.7154	133.0199

Table 7. Goodness-of-fit statistics for Dataset I.

Model	K-S	p-value	W^2	A^2
UDFWD	0.0418	0.9996	0.0168	0.1551
ENH	0.0518	0.9910	0.0343	0.2528
MKW	0.0562	0.9782	0.0345	0.2748
KwW	0.0398	0.9999	0.0157	0.1462
EEW	0.0395	0.9999	0.0154	0.1435
TLIW	0.1176	0.2785	0.2617	1.7343
IW	0.1336	0.1570	0.4137	2.7243

Among the competing models in Table 6, the UDFWD gives the smallest AIC, AICc, BIC, CAIC, and HQIC values. However, the goodness-of-fit statistics do not show the same ranking. Slightly smaller K–S, W^2, and A^2 values are obtained for the EEW and KwW models, although the differences from the UDFWD are small. Thus, the UDFWD remains competitive in terms of the distance-based goodness-of-fit measures.

The fitted PDFs of all competing models are shown in Figure 7, while the corresponding P–P and Q–Q plots are presented in Figure 8. The fitted UDFWD curve follows the general shape of the histogram. Its P–P and Q–Q points also lie close to the reference diagonal, indicating good agreement between the fitted distribution and the observed data.

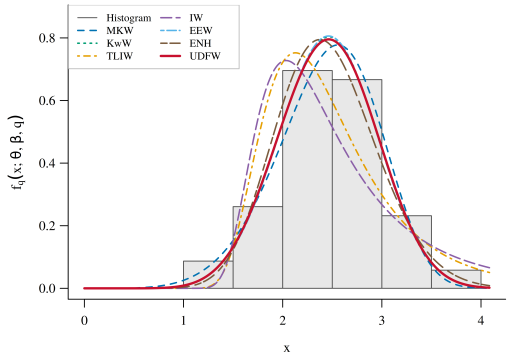
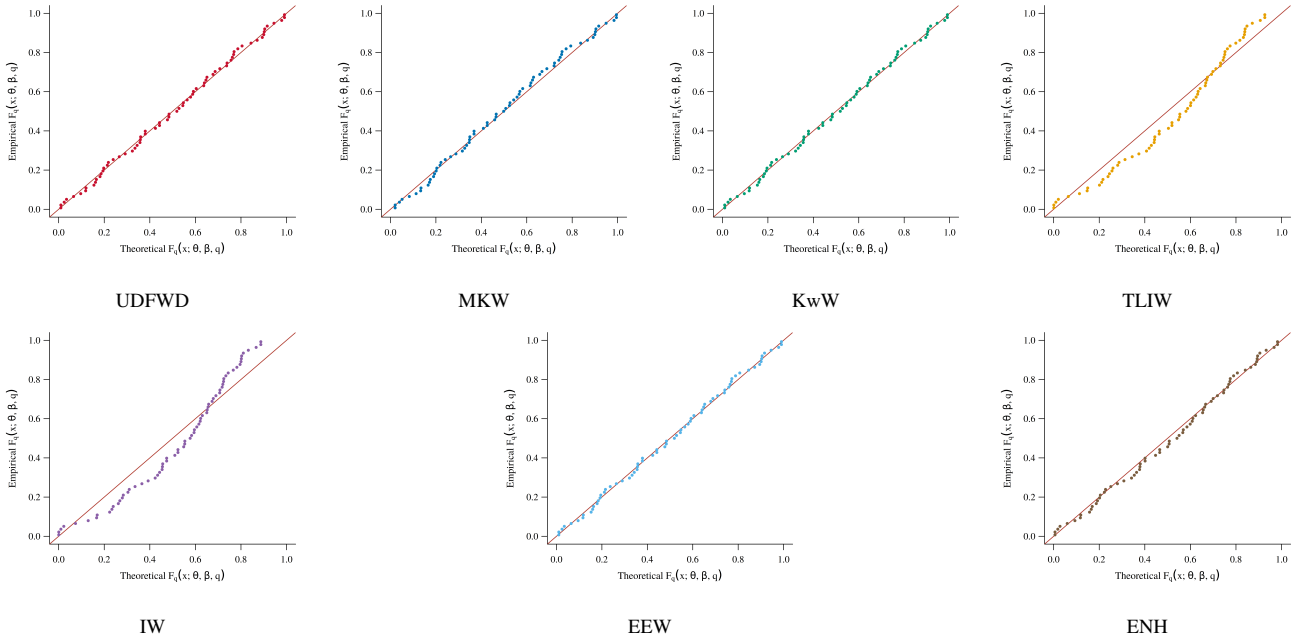
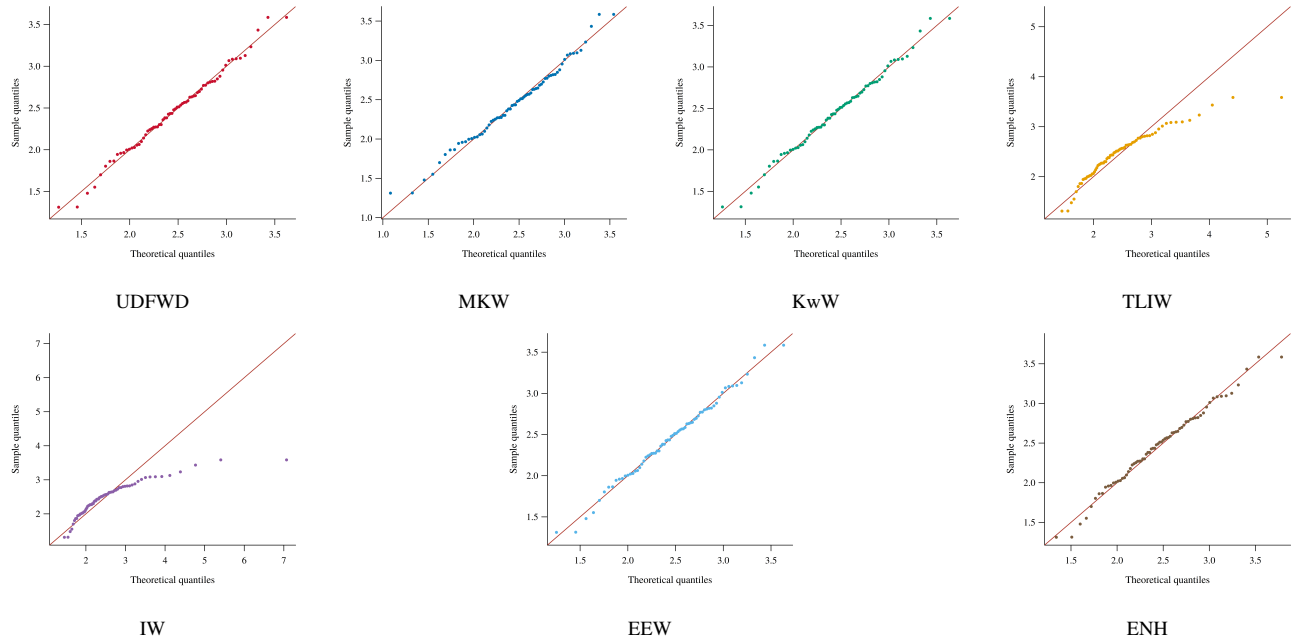


Figure 7. Fitted PDFs of the competing models.



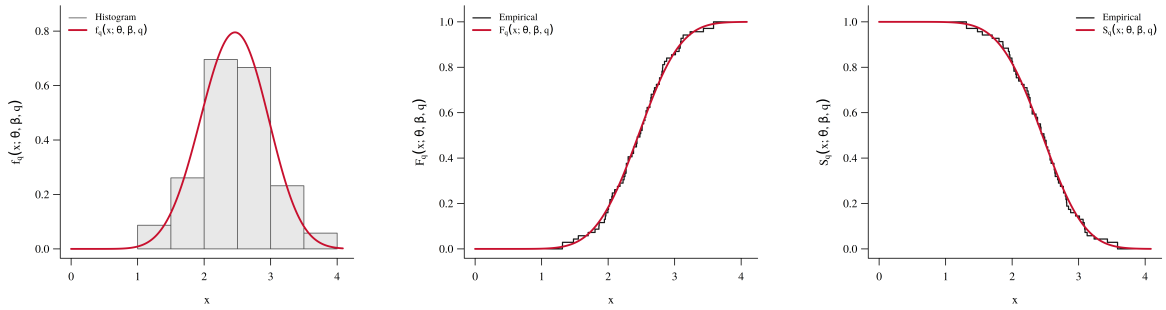
(a) P–P plots of the competing models.



(b) Q–Q plots of the competing models.

Figure 8. Model-comparison diagnostics for Dataset I.

For a closer view of the proposed model, the fitted UDFWD PDF, CDF, and survival function are shown in Figure 9. These plots show close agreement between the empirical curves and the fitted UDFWD model.



(a) Fitted PDF. **(b)** Fitted CDF. **(c)** Fitted survival function.

Figure 9. Empirical and fitted UDFWD functions for Dataset I.

5.2. Dataset II: Biomedical serum creatinine data

The second dataset consists of $n = 19$ serum creatinine measurements, as reported in [29]. Serum creatinine is commonly used in clinical biomarkers to assess kidney function and detect possible renal impairment. The data are as follows:

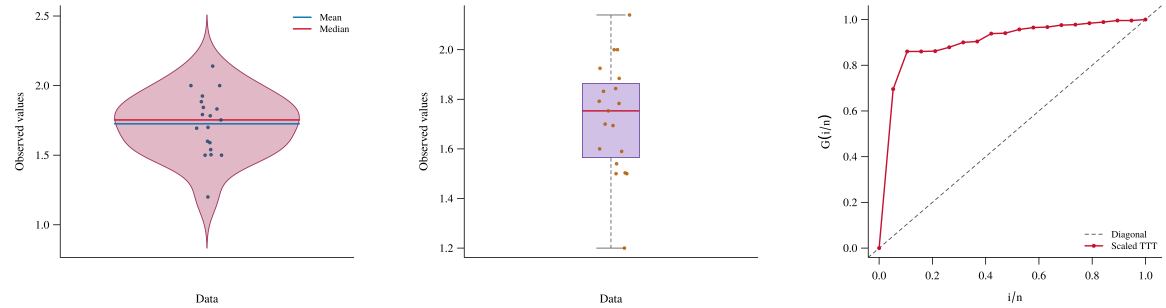
$$1.925,\ 1.500,\ 2.000,\ 1.600,\ 1.700,\ 1.7533,\ 1.540,\ 1.694,\ 1.8843,$$
$$1.8433,\ 1.832,\ 1.590,\ 1.7833,\ 1.200,\ 1.792,\ 1.500,\ 1.5033,\ 2.000,\ 2.140.$$

The summary statistics are reported in Table 8.

Table 8. Summary statistics for Dataset II.

n	Min.	Q_1	Median	Mean	Q_3	Max.	SD	Variance	Skewness	Kurtosis
19	1.200	1.565	1.7533	1.7253	1.8638	2.140	0.2259	0.0510	-0.3310	3.2712

The observations fall within a short interval, from 1.200 to 2.140. The mean and the median are close. The skewness is negative, which means that the data are slightly skewed to the left. The violin, box, and TTT plots are displayed in Figure 10. As in Dataset I, the TTT curve is concave and lies above the diagonal line, an empirical pattern typically associated with an increasing hazard rate and consistent with the IFR property of the fitted UDFWD.



(a) Violin plot. **(b)** Box and strip plot. **(c)** TTT plot.

Figure 10. Exploratory plots for Dataset II.

The MLEs and model selection criteria for Dataset II are reported in Table 9, whereas the goodness-of-fit statistics are reported in Table 10.

Table 9. MLEs and model selection criteria for Dataset II.

Model	Estimates	$-\ell$	AIC	AICc	BIC	CAIC	HQIC
UDFWD	$\widehat{\theta} = 6.4528$, $\widehat{\beta} = 0.0177$, $\widehat{q} = 0.4479$	-1.9994	2.0012	3.6012	4.8345	7.8345	2.4807
MKW	$\widehat{\alpha} = 0.6897$, $\widehat{\beta} = 0.0083$, $\widehat{\gamma} = 785.1100$	-1.9018	2.1964	3.7964	5.0298	8.0298	2.6760
ENH	$\widehat{\alpha} = 1.4529 \times 10^{-5}$, $\widehat{\gamma} = 65673.1686$, $\widehat{\lambda} = 42.1716$	-1.2283	3.5434	5.1434	6.3768	9.3768	4.0229
KwW	$\widehat{\delta}_1 = 1.6531$, $\widehat{\delta}_2 = 0.1485$, $\widehat{\gamma} = 0.0591$, $\widehat{\theta} = 8.0840$	-2.0184	3.9632	6.8203	7.7409	11.7409	4.6025
EEW	$\widehat{c} = 6.8793$, $\widehat{\beta} = 2.4635$, $\widehat{\alpha} = 1.6613$, $\widehat{\lambda} = 11.8171$	-1.9930	4.0141	6.8712	7.7919	11.7919	4.6534
TLIW	$\widehat{\alpha} = 1.8917$, $\widehat{\beta} = 5.4266$, $\widehat{\lambda} = 0.5628$	0.6577	7.3154	8.9154	10.1487	13.1487	7.7949
IW	$\widehat{\eta} = 6.5837$, $\widehat{\gamma} = 21.5540$	2.2058	8.4116	9.1616	10.3005	12.3005	8.7313

Table 10. Goodness-of-fit statistics for Dataset II.

Model	K–S	p-value	W^2	A^2
UDFWD	0.1005	0.9865	0.0238	0.1856
MKW	0.1081	0.9716	0.0257	0.1973
ENH	0.1153	0.9503	0.0368	0.2890
KwW	0.1028	0.9828	0.0234	0.1865
EEW	0.0999	0.9874	0.0240	0.1855
TLIW	0.1491	0.7578	0.0770	0.5964
IW	0.1720	0.5861	0.1159	0.8662

Table 9 shows that the proposed UDFWD gives the smallest AIC, AICc, BIC, CAIC, and HQIC values. Table 10 shows that EEW gives the smallest K-S and A^2 values, whereas KwW gives the smallest W^2 value. However, the UDFWD values are almost identical to the best values. Therefore, the proposed model remains highly competitive according to the distance-based goodness-of-fit measures.

The fitted PDFs and the P–P and Q–Q plots for all competing models are presented in Figures 11 and 12. The UDFWD curve follows the main pattern of the histogram, and its P–P and Q–Q points remain close to the diagonal line.

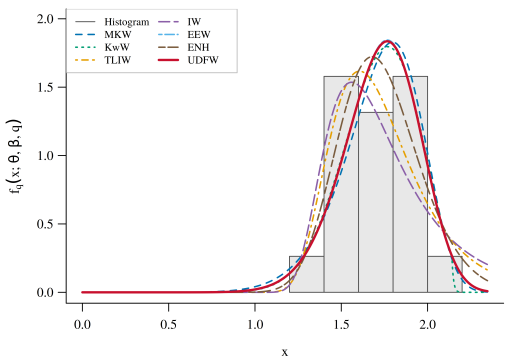
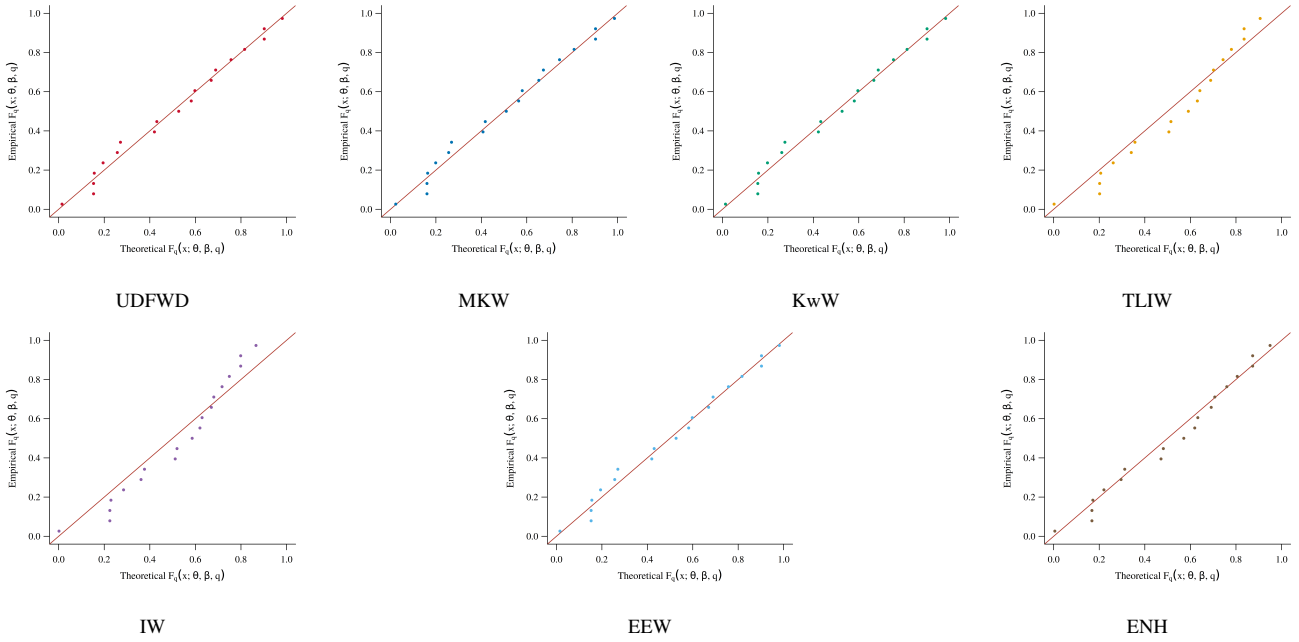
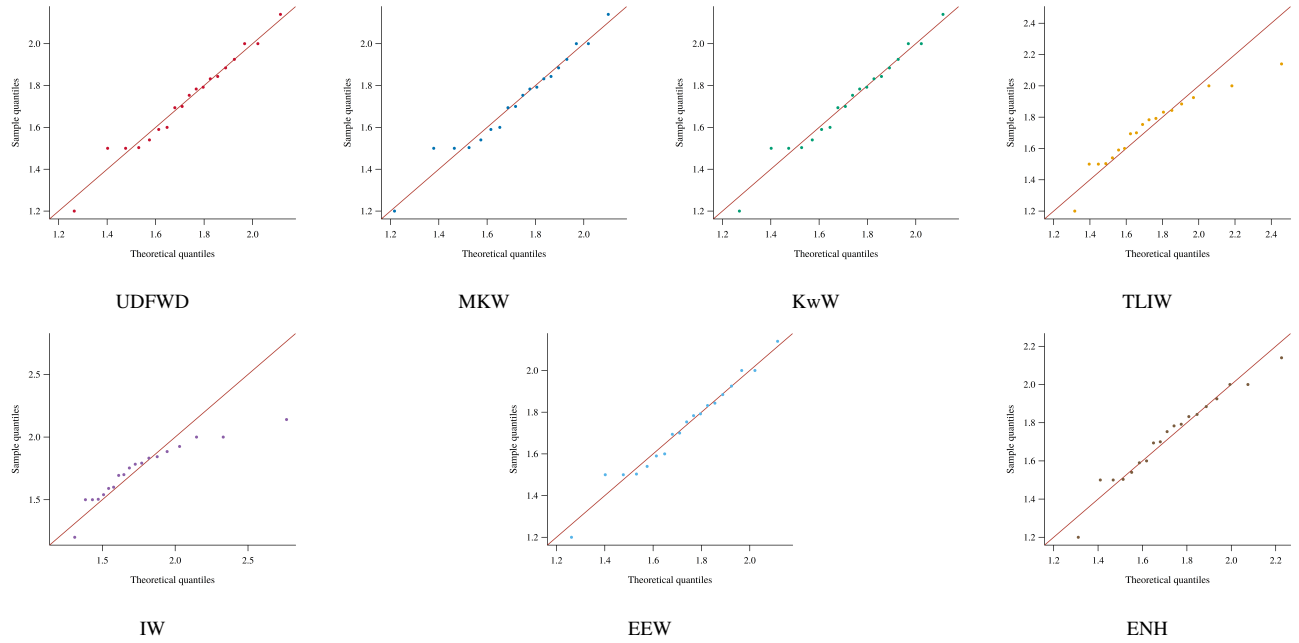


Figure 11. Fitted PDFs of the competing models.



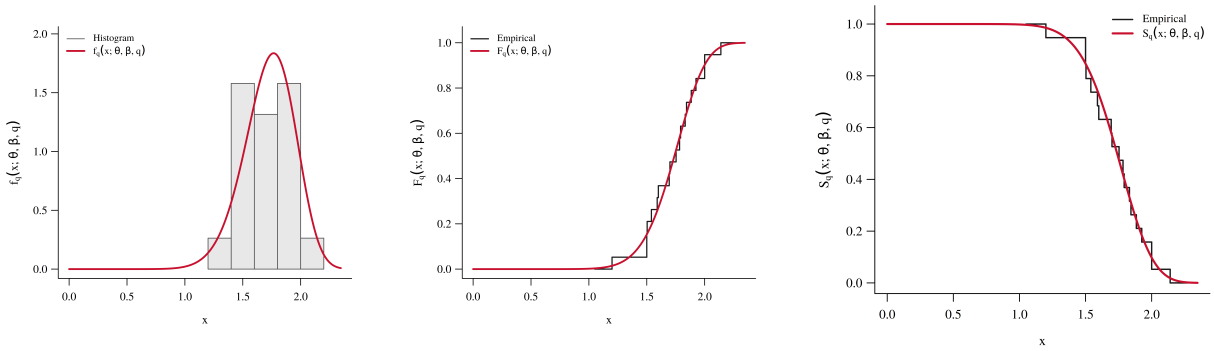
(a) P–P plots of the competing models.



(b) Q–Q plots of the competing models.

Figure 12. Model-comparison diagnostics for Dataset II.

For a closer view of the proposed model, the fitted UDFWD PDF, CDF, and survival function are shown in Figure 13. These plots show good agreement between the empirical curves and the fitted UDFWD model.



(a) Fitted PDF. **(b)** Fitted CDF. **(c)** Fitted survival function.

Figure 13. Empirical and fitted UDFWD functions for Dataset II.

5.3. Discussion

The two applications show that the proposed UDFWD is flexible for modeling positive continuous data from engineering reliability and biomedical fields. For Dataset I, the UDFWD gives the smallest information-criterion values, and its distance-based goodness-of-fit measures remain very close to those of the best competing models. For Dataset II, the UDFWD again yields the smallest information-criterion values and distance-based measures, which are almost identical to the best values.

The favorable performance of the UDFWD appears to arise from the additional distributional flexibility introduced by q through changes in concentration and tail behavior. However, because the distance-based goodness-of-fit measures differ only slightly from the best competing models, the practical gain in empirical fit over the closest alternatives is modest.

This difference is not contradictory. The two groups of criteria assess model performance from different perspectives. Information criteria balance model fit and complexity by penalizing additional model complexity, which is particularly important because the additional parameter q may increase the risk of overfitting in small or moderate samples.

The AICc adjusts AIC for sample size, which matters here because Dataset II contains only $n = 19$ observations. The K–S, W^2, and A^2 statistics, together with the P–P and Q–Q plots, assess a different aspect of the fit, namely how closely the fitted distribution agrees with the observed data, and which criterion is most appropriate depends on the aim of the study.

The estimated fractional parameter is $\widehat{q} = 0.3255$ for Dataset I and $\widehat{q} = 0.4479$ for Dataset II, both below the boundary value $q = 1$ that corresponds to the classical WD. These estimates are interpreted descriptively only, and no formal inferential conclusion is drawn about whether the fitted model differs from the Weibull submodel.

Overall, the fitted PDF, the fitted CDF, and the fitted survival function, along with the P–P and Q–Q plots, confirm the numerical results obtained in this study. Taken together, they indicate close agreement between the proposed model and the observed data. The UDFWD may thus be regarded as a useful and competitive model for positive continuous data in engineering reliability applications and in biomedical fields.

6. Conclusions

This paper introduced the UDFWD, obtained by replacing the ordinary derivative in the differential equation associated with the density of the classical WD by the UDF derivative of order $q \in (0, 1]$. A series representation of the normalizing constant was derived and shown to be absolutely convergent for $\theta > 1$, and series expressions were obtained for the cumulative distribution, survival, and hazard functions in terms of the gamma and incomplete gamma functions. The classical WD is recovered as $q \to 1^-$. The density was further proved to be strictly log-concave for $\theta > 1, \beta > 0$, and $0 < q \leq 1$, so that the model has a strictly increasing hazard rate and a unique mode, with q governing the level and growth of the hazard through the factor $1/q$ and the additive constant $(1 - q)/q$. The mode; quantile function; moments; and Shannon, Tsallis, and Rényi entropies were also derived. The parameters were estimated by the maximum likelihood, least squares, and weighted least squares methods. The simulation results showed that the three methods become more accurate as the sample size increases. For moderate and large sample sizes, the MLE yields the smallest MSEs in most cases. In both applications, the UDFWD gives the smallest values of all model-selection criteria. It also remains highly competitive in terms of the distance-based measures. The scaled TTT transforms of the two datasets are concave, which agrees with the increasing failure rate proved analytically. However, the extra flexibility of the UDFWD comes with a higher computational cost. In small samples, the fractional parameter may also be estimated with less precision. Therefore, when the fitted value of q is close to one, and the classical WD fits the data adequately, the simpler WD may still be preferred for reasons of parsimony and computational efficiency. As future work, the proposed model may be extended to censored data, regression formulations, and Bayesian inference, and fractional versions of other lifetime distributions can be derived by following the same approach.

Author contributions

Nesreen M. Al-Olaimat: Conceptualization, methodology, formal analysis, software, validation, data curation, visualization, writing—original draft, writing—review and editing; Hatim Solayman Migdadi: Formal analysis, software, data curation, visualization, writing—original draft; Afaf Alrashidi: Validation, writing—review and editing; Samirah Alzubaidi: Validation, writing—review and editing. All authors have read and approved the final manuscript.

Use of Generative-AI tools declaration:

The authors declare that they have not used Artificial Intelligence (AI) tools in the creation of this article.

Acknowledgments

The authors extend their appreciation to Umm Al-Qura University, Saudi Arabia for funding this research work through grant number: 26UQU4340101GSSR07.

Funding

This research work was funded by Umm Al-Qura University, Saudi Arabia under grant number: 26UQU4340101GSSR07.

Data Availability

All relevant data are within the paper, and references for the data are mentioned.

Conflict of interest

The authors have declared that no competing interests exist.

References

1. H. Wu, X. Guo, W. Sun, L. K. Song, Q. Deng, S. Yang, et al., Fatigue life prediction of steels in hydrogen environments using physics-informed learning, *Appl. Sci.*, **16** (2026), 1905. https://doi.org/10.3390/app16041905
2. F. Laganà, Design and simulation-based validation of an embedded acquisition architecture for in situ PCB integrity monitoring in biomedical devices, *Electronics*, **15** (2026), 833. https://doi.org/10.3390/electronics15040833
3. W. Weibull, A statistical distribution function of wide applicability, *J. Appl. Mech.*, **18** (1951), 293–297. https://doi.org/10.1115/1.4010337
4. G. S. Mudholkar, D. K. Srivastava, Exponentiated Weibull family for analyzing bathtub failure-rate data, *IEEE Trans. Reliab.*, **42** (1993), 299–302. https://doi.org/10.1109/24.229504
5. C. D. Lai, M. Xie, D. N. P. Murthy, A modified Weibull distribution, *IEEE Trans. Reliab.*, **52** (2003), 33–37. https://doi.org/10.1109/TR.2002.805788
6. Y. Y. Abdelall, A. S. Hassan, E. M. Almetwally, A new extention of the odd inverse Weibull-G family of distributions: Bayesian and non-Bayesian estimation with engineering applications, *Comput. J. Math. Stat. Sci.*, **3** (2024), 359–388. https://doi.org/10.21608/CJMSS.2024.285399.1050
7. M. Bebbington, C. D. Lai, R. Zitikis, A flexible Weibull extension, *Reliab. Eng. Syst. Saf.*, **92** (2007), 719–726. https://doi.org/10.1016/j.ress.2006.03.004
8. M. E. Ghitany, E. K. Al-Hussaini, R. A. Al-Jarallah, Marshall-Olkin extended Weibull distribution and its application to censored data, *J. Appl. Stat.*, **32** (2005), 1025–1034. https://doi.org/10.1080/02664760500165008
9. G. M. Cordeiro, E. M. M. Ortega, S. Nadarajah, The Kumaraswamy Weibull distribution with application to failure data, *J. Franklin Inst.*, **347** (2010), 1399–1429. https://doi.org/10.1016/j.jfranklin.2010.06.010
10. G. R. Aryal, C. P. Tsokos, Transmuted Weibull distribution: a generalization of the Weibull probability distribution, *Eur. J. Pure Appl. Math.*, **4** (2011), 89–102.

11. M. Nassar, A. Alzaatreh, M. Mead, O. Abo-Kasem, Alpha power Weibull distribution: properties and applications, *Commun. Stat. Theory Methods*, **46** (2017), 10236–10252. https://doi.org/10.1080/03610926.2016.1231816
12. M. S. Shama, A. S. Alharthi, F. A. Almulhim, A. M. Gemeay, M. A. Meraou, M. S. Mustafa, et al., Modified generalized Weibull distribution: theory and applications, *Sci. Rep.*, **13** (2023), 12828. https://doi.org/10.1038/s41598-023-38942-9
13. H. M. Alshanbari, O. H. Odhah, H. Al-Mofleh, Z. Ahmad, S. K. Khosa, A. A. H. El-Bagoury, A new flexible Weibull extension model: different estimation methods and modeling an extreme value data, *Heliyon*, **9** (2023), e21704. https://doi.org/10.1016/j.heliyon.2023.e21704
14. W. Emam, On statistical modeling using a new version of the flexible Weibull model: Bayesian, maximum likelihood estimates, and distributional properties with applications in the actuarial and engineering fields, *Symmetry*, **15** (2023), 560. https://doi.org/10.3390/sym15020560
15. R. Alotaibi, H. Okasha, M. Nassar, A. Elshahhat, A novel modified alpha power transformed Weibull distribution and its engineering applications, *Comput. Model. Eng. Sci.*, **135** (2023), 2065–2089. https://doi.org/10.32604/cmes.2023.023408
16. F. Hernández-Barajas, O. Usuga-Manco, C. Patino-Rodríguez, F. Marmolejo-Ramos, Distributional modelling of positively skewed data via the flexible Weibull extension distribution, *Aust. N. Z. J. Stat.*, **66** (2024), 306–324. https://doi.org/10.1111/anzs.12423
17. A. Z. Afify, R. Alsultan, A. S. Alghamdi, H. A. Mahran, A new flexible Weibull distribution for modeling real-life data: improved estimators, properties, and applications, *AIMS Math.*, **10** (2025), 5880–5927. https://doi.org/10.3934/math.2025270
18. A. M. Mathai, Statistical distribution theory and fractional calculus, *Stats*, **7** (2024), 1259–1295. https://doi.org/10.3390/stats7040074
19. A. Abuualshaikh, M. Z. Aldrabseh, T. S. Alshammari, K. A. Rashedi, K. M. K. Alshammari, A new generalized differential transform method for fractional ODEs with statistical applications, *AIMS Math.*, **11** (2026), 9541–9562. https://doi.org/10.3934/math.2026395
20. A. Di Crescenzo, A. Meoli, On a fractional alternating Poisson process, *AIMS Math.*, **1** (2016), 212–224. https://doi.org/10.3934/Math.2016.3.212
21. M. Abu Hammad, A. Awad, R. Khalil, Properties of conformable fractional chi-square probability distribution, *J. Math. Comput. Sci.*, **10** (2020), 1239–1250. https://doi.org/10.28919/jmcs/4583
22. A. Dixit, A. Ujlayan, P. Ahuja, On the properties of the UD differential and integral operator, *Math. Eng. Sci. Aerosp.*, **11** (2020), 291–300.
23. A. Dixit, A. Ujlayan, The theory of UD derivative and its applications, *TWMS J. Appl. Eng. Math.*, **11** (2021), 350–358.
24. I. Alhribat, M. H. Samuh, Generating statistical distributions using fractional differential equations, *Jordan J. Math. Stat.*, **16** (2023), 379–396. https://doi.org/10.47013/16.2.11
25. A. Jamal, I. Alhribat, M. H. Samuh, Generating novel probability distributions: a UD fractional derivative approach, *J. Stat. Res.*, **58** (2024), 279–298. https://doi.org/10.3329/jsr.v58i2.80609

26. N. M. Al-Olaimat, M. A. Amleh, B. Abughazaleh, R. Saadeh, M. Hafez, Statistical applications of the Ujlayan-Dixit fractional Lomax probability distribution, *Fractal Fract.*, **10** (2026), 155. https://doi.org/10.3390/fractalfract10030155

27. G. Derflinger, W. Hörmann, J. Leydold, Random variate generation by numerical inversion when only the density is known, *ACM Trans. Model. Comput. Simul.*, **20** (2010), 1–25. https://doi.org/10.1145/1842722.1842723

28. W. J. Padgett, S. D. Durham, A. M. Mason, Weibull analysis of the strength of carbon fibers using linear and power law models for the length effect, *J. Compos. Mater.*, **29** (1995), 1873–1884. https://doi.org/10.1177/002199839502901405

29. M. E. Qura, A. Fayomi, M. Kilai, E. M. Almetwally, Bivariate power Lomax distribution with medical applications, *PLoS ONE*, **18** (2023), e0282581. https://doi.org/10.1371/journal.pone.0282581

Appendix

A. Convergence of the series representation

Here, we establish the absolute convergence of the infinite series appearing in the normalizing constant in Eq (2.3). Consider the ratio of two consecutive absolute terms of the series

$$\frac{\frac{\left|-\frac{1-q}{q}\left(\frac{\beta}{q}\right)^{-\frac{1}{\theta}}\right|^{j+1}}{(j+1)!}\Gamma\left(\frac{\theta+q(j+2)-1}{q\theta}\right)}{\frac{\left|-\frac{1-q}{q}\left(\frac{\beta}{q}\right)^{-\frac{1}{\theta}}\right|^{j}}{j!}\Gamma\left(\frac{\theta+q(j+1)-1}{q\theta}\right)}. \tag{A.1}$$

After simplification, Eq (A.1) becomes

$$\frac{\left|-\frac{1-q}{q}\left(\frac{\beta}{q}\right)^{-\frac{1}{\theta}}\right|}{j+1}\cdot\frac{\Gamma\left(\frac{\theta+q(j+2)-1}{q\theta}\right)}{\Gamma\left(\frac{\theta+q(j+1)-1}{q\theta}\right)}.$$

Using the asymptotic relation

$$\frac{\Gamma(y+r)}{\Gamma(y)}\sim y^{r}, \qquad y\to\infty,$$

we obtain

$$\frac{\left|-\frac{1-q}{q}\left(\frac{\beta}{q}\right)^{-\frac{1}{\theta}}\right|}{j+1}\cdot\frac{\Gamma\left(\frac{\theta+q(j+2)-1}{q\theta}\right)}{\Gamma\left(\frac{\theta+q(j+1)-1}{q\theta}\right)}\sim\left|\frac{1-q}{q}\left(\frac{\beta}{q}\right)^{-\frac{1}{\theta}}\right|\theta^{-\frac{1}{\theta}}j^{\frac{1}{\theta}-1}.$$

If $\theta>1$, then

$$\frac{1}{\theta}-1<0.$$

Therefore,

$$\lim_{j\to\infty}\left[\left|\frac{1-q}{q}\left(\frac{\beta}{q}\right)^{-\frac{1}{\theta}}\right|\theta^{-\frac{1}{\theta}}j^{\frac{1}{\theta}-1}\right]=0. \tag{A.2}$$

Hence, the series in (2.3) is absolutely convergent for $\theta > 1$.

B. Convergence of the series in the Tsallis and Rényi entropy measures

Let a_j denote the absolute value of the jth term of the series appearing in Eqs (3.9) and (3.10). For $0 < q < 1$, the ratio of two consecutive terms satisfies

$$\frac{a_{j+1}}{a_j}=\frac{\delta(1-q)}{q(j+1)}\left(\frac{\delta\beta}{q}\right)^{-\frac{1}{\theta}}\frac{\Gamma\left(\frac{\delta(\theta-1)+q(j+2)}{q\theta}\right)}{\Gamma\left(\frac{\delta(\theta-1)+q(j+1)}{q\theta}\right)}.$$

Using the asymptotic relation

$$\frac{\Gamma(z+a)}{\Gamma(z)}\sim z^a, \qquad z\to\infty,$$

we obtain

$$\frac{a_{j+1}}{a_j}\sim\frac{\delta(1-q)}{q\theta^{1/\theta}}\left(\frac{\delta\beta}{q}\right)^{-\frac{1}{\theta}}j^{\frac{1}{\theta}-1}.$$

Because $\theta > 1$, we have

$$\frac{1}{\theta}-1<0,$$

and hence,

$$\lim_{j\to\infty}\frac{a_{j+1}}{a_j}=0.$$

Therefore, the series is absolutely convergent. When $q = 1$, the coefficient $(1-q)^j$ vanishes for every $j \geq 1$, and hence, the series reduces to its first term.

Moreover, near zero, the integrand $f_q^{\delta}(x;\theta,\beta,q)$ behaves as

$$x^{\frac{\delta(\theta-1)}{q}},$$

which is integrable because $\delta > 0$, $\theta > 1$, and $q > 0$. As $x \to \infty$, the exponential factor

$$e^{\left(-\frac{\delta\beta}{q}x^{\theta}\right)}$$

ensures integrability. Consequently, the interchange of summation and integration is justified, and the Tsallis and Rényi entropy measures are well-defined for $\delta > 0$, $\delta \neq 1$, $\beta > 0$, $\theta > 1$, and $0 < q \leq 1$.

AIMS Press

© 2026 the Author(s), licensee AIMS Press. This is an open access article distributed under the terms of the Creative Commons Attribution License (http://creativecommons.org/licenses/by/4.0)